

DOCUMENT CONTROL DATA - R & D

(Security classification of title, body of abstract and indexing annotation must be entered when the overall report is classified)

1. ORIGINATING ACTIVITY (Corporate author)		2a. REPORT SECURITY CLASSIFICATION	
Naval Research Laboratory Washington, D.C. 20390		Unclassified	
		2b. GROUP	
3. REPORT TITLE			
DYNAMIC TEAR TEST INVESTIGATIONS OF THE FRACTURE TOUGHNESS OF THICK-SECTION STEEL—HEAVY SECTION STEEL TECHNOLOGY PROGRAM TECHNICAL REPORT 7			
4. DESCRIPTIVE NOTES (Type of report and inclusive dates)			
Final summary report on the NRL Problem.			
5. AUTHOR(S) (First name, middle initial, last name)			
F. J. Loss			
6. REPORT DATE		7a. TOTAL NO. OF PAGES	7b. NO. OF REFS
May 14, 1970		54	12
8a. CONTRACT OR GRANT NO.		9a. ORIGINATOR'S REPORT NUMBER(S)	
NRL Problem M01-14		NRL Report 7056	
b. PROJECT NO.			
AEC-83-Y-80507V			
c.		9b. OTHER REPORT NO(S) (Any other numbers that may be assigned this report)	
d.		Heavy Section Steel Technology Program Technical Report HSSTP-TR-7	
10. DISTRIBUTION STATEMENT			
This document has been approved for public release and sale; its distribution is unlimited.			
11. SUPPLEMENTARY NOTES		12. SPONSORING MILITARY ACTIVITY	
U.S. Atomic Energy Commission, Heavy Section Steel Technology Program, Oak Ridge, Tenn. 37830		See item 11 for nonmilitary sponsor	
13. ABSTRACT			
<p>The effect of mechanical constraint imposed by thick sections is examined in the framework of linear elastic fracture mechanics (LEFM) and other temperature-transition indices. Extrapolation of thin-section LEFM data to higher temperatures has raised the concern that thick-section steels, of shelf toughness and strength class similar to A533-B, will not exhibit a brittle-to-ductile transition with increasing temperature. Research programs at NRL relating to thick dynamic tear (DT) test studies and those at Westinghouse relating to thick LEFM investigations have shown that unirradiated A533-B does exhibit a significant increase in toughness within a relatively narrow temperature region near the nil ductility transition (NDT) temperature. Size effects studies indicate that the effects of mechanical constraint associated with thick sections elevate the fracture transition—elastic (FTE) temperature (the temperature at which very large flaws remain dormant up to yield stress) for 12-in.-thick sections approximately 70°F (39°C) above the FTE temperature for thin sections, which in turn is 60°F (33°C) above the NDT temperature. For the steels investigated the DT energy curve may be divided into three toughness regimes which are shown to indicate similar transition features for specimens of 5/8-in. to 12-in. thickness. Regime 1 defines a temperature interval of rapidly increasing dynamic LEFM fracture toughness which eventually renders this technique inapplicable with small increases in temperature. Regime 3 represents fractures exhibiting large plastic deformation for which suitable fracture mechanics analyses have not yet been developed. Regime 2 defines a transition between the two extreme cases in which nominal stresses above yield level become necessary to propagate fracture. The mid-point energy, located in this regime, is defined as the FTE for steels of A533 toughness level.</p>			

14. KEY WORDS	LINK A		LINK B		LINK C	
	ROLE	WT	ROLE	WT	ROLE	WT
Fracture-safe design Structural steels A533-B steel Thick section steels Nuclear pressure vessels Fracture toughness tests Transition temperature for steel Fracture mechanics tests Dynamic tear test Size effect Mechanical constraint Through-thickness metallurgical variations Thick section weldment						

CONTENTS

Abstract	ii
Problem Status	ii
Authorization	ii
INTRODUCTION	1
DYNAMIC TEAR TEST PROCEDURES	2
MATERIAL PROPERTIES	7
THROUGH-THICKNESS FRACTURE TOUGHNESS VARIATIONS FOR PLATES AND WELDMENTS	9
12-in. A533-B Class 1 Plates Toughness to 600°F (316°C)	9 14
6-in. A533-B Class 2 Plate	16
12-in. A533 Submerged Arc Weld	19
6-in. A533 Electroslag Weld	20
THICK SECTION DT STUDIES	21
1-in. DT Investigations	21
3-in. DT Investigations	22
6-in. DT Investigations	26
12-in. DT Investigations	29
SIZE EFFECT INTERPRETATIONS	33
COMPARISON OF DT TESTS WITH FRACTURE MECHANICS	37
SUMMARY	39
REFERENCES	40
APPENDIX A – Tabulations of the Data	41

ABSTRACT

The effect of mechanical constraint imposed by thick sections is examined in the framework of linear elastic fracture mechanics (LEFM) and other temperature-transition indices. Extrapolation of thin-section LEFM data to higher temperatures has raised the concern that thick-section steels, of shelf toughness and strength class similar to A533-B, will not exhibit a brittle-to-ductile transition with increasing temperature. Research programs at NRL relating to thick dynamic tear (DT) test studies and those at Westinghouse relating to thick LEFM investigations have shown that unirradiated A533-B does exhibit a significant increase in toughness within a relatively narrow temperature region near the nil ductility transition (NDT) temperature. Size effects studies indicate that the effects of mechanical constraint associated with thick sections elevate the fracture transition — elastic (FTE) temperature (the temperature at which very large flaws remain dormant up to yield stress) for 12-in.-thick sections approximately 70°F (39°C) above the FTE temperature for thin sections, which in turn is 60°F (33°C) above the NDT temperature. For the steels investigated the DT energy curve may be divided into three toughness regimes which are shown to indicate similar transition features for specimens of 5/8-in. to 12-in. thickness. Regime 1 defines a temperature interval of rapidly increasing dynamic LEFM fracture toughness which eventually renders this technique inapplicable with small increases in temperature. Regime 3 represents fractures exhibiting large plastic deformation for which suitable fracture mechanics analyses have not yet been developed. Regime 2 defines a transition between the two extreme cases in which nominal stresses above yield level become necessary to propagate fracture. The midpoint energy, located in this regime, is defined as the FTE for steels of A533 toughness level.

PROBLEM STATUS

This is a final report on one phase of this problem.

AUTHORIZATION

NRL Problem M01-14
AEC-83-Y-80507V

Manuscript submitted January 20, 1970.

DYNAMIC TEAR TEST INVESTIGATIONS OF THE
FRACTURE TOUGHNESS OF THICK-SECTION STEEL

HEAVY SECTION STEEL TECHNOLOGY PROGRAM
TECHNICAL REPORT 7

INTRODUCTION

The Heavy Section Steel Technology (HSST) Program came into being primarily as a result of a 1965 letter (1) by the Advisory Committee on Reactor Safeguards (ACRS) to the U.S. Atomic Energy Commission (AEC). This letter stated that to reduce the already small probability of pressure vessel failure the industry and the AEC should further consider improvement of means for evaluating factors that may affect the nil ductility transition (NDT) temperature. The NDT constitutes an important index value for the temperature-induced transition in the fracture resistance of reactor pressure vessel steels. The NDT approach interprets the sharp increase in fracture toughness over a limited temperature interval in terms of a corresponding increase in critical flaw size for a given stress level. The Fracture Analysis Diagram (FAD) evolved from service failures defines that very large flaws will remain dormant up to yield stress loads at temperatures above the NDT temperature plus 60°F (33°C) for steels of relatively thin section (2). The temperature corresponding to the NDT temperature plus 60°F (33°C) is classified as the FTE (fracture transition — elastic) temperature. The applicable FTE temperature for very thick sections remained in question at that time; however, the general premise derived from metallurgical concepts was that the effect of section size in elevating the FTE should be limited by the microfracture ductility transition.

Interpretations of linear elastic fracture mechanics (LEFM) data existing at the time the HSST Program was initiated led to the postulation that thick sections may not exhibit the expected sharp increase in toughness in the transition temperature region. Fracture mechanics K_{Ic} values for low-alloy steels as obtained with 1- and 2-in.-thick specimens were available only at temperatures below NDT. Valid data according to ASTM Committee E-24 could not be obtained at higher temperatures because the thickness used was insufficient to maintain plane strain constraint. It was postulated that the increased mechanical constraint associated with thicker specimens would enable valid LEFM data to be obtained to relatively high temperatures beyond the transition temperature region. K_{Ic} values in this high-temperature region were thereupon projected by a linear extrapolation of the existing data. If the extrapolation was correct, catastrophic failure near reactor operating temperatures could be postulated from surface flaws of a few inches depth in regions of stress concentration for vessels under nominal elastic loads.

These fracture mechanics projections do not address themselves to the metallurgical processes taking place in the transition temperature region. Other investigators believed that the effects of microfracture processes were not eliminated by thickness-induced constraint. The metallurgical viewpoint predicted that a sharp increase in toughness would be observed for thick sections, even though this behavior might be displaced to moderately higher temperatures due to the mechanical constraint.

The initial efforts of these studies under the HSST Program were aimed at resolving this critical research question. Experimental programs were undertaken at NRL to examine the transition temperature aspects of A533-B steel and at Westinghouse Research

Laboratories to investigate the LFM behavior of the same steel. Both programs were to use specimens up to 12 in. thick. The NRL investigations centered on the dynamic tear (DT) test, while those at Westinghouse employed the compact tension specimen (CTS).

The NRL program was funded internally as well as by the HSST Program. Under HSST funding, investigations of the fracture toughness through the thickness of four 12-in.-thick plates and weldments of A533-B steel were conducted with 5/8-in. DT specimens. Thickness effects due to mechanical constraint were investigated with three different sizes of DT specimens from 5/8-in. to 3-in. thick. An investigation of the DT behavior of 12-in.-thick specimens from one plate of A533-B Class 1 (HSST 01) supplied by the HSST Program was conducted under the NRL program. Another NRL-funded portion included a full-thickness DT investigation on a 6-in.-thick A533-B Class 2 plate purchased by NRL. This study was extended to include variations in fracture toughness through the thickness using 5/8-in. DT specimens.

The primary objective of the NRL research was to demonstrate the reality of the existence of a sharp increase in toughness for thick section steels in the transition temperature region as defined by thinner sections. Since these investigations were oriented primarily to the transition temperature region, the effects of plasticity at the high temperature end of the transition were not a primary area of research. Existence of high plastic strains related to through-thickness yielding provides direct evidence that catastrophic failure could not occur under elastic loads. Such evidence also indicates that LFM limits of applicability are exceeded.

DYNAMIC TEAR TEST PROCEDURES

The basic DT test procedure consists of impacting a simple supported specimen having a specially prepared brittle electron-beam (EB) crack starter weld on the tension side (Fig. 1). Six different specimens are currently in use. These range in thickness from 5/8 in. to 12 in. (Fig. 2 and Table 1). The dimensions of a special 10-in. DT specimen to be discussed later are also listed. An alternate notch preparation for the 5/8-in. specimen uses a deep machined notch with the tip sharpened by a pressed knife edge. The specimens are fractured on either pendulum or drop-weight machines, and the energy absorbed during the fracture process is recorded. The 5/8-in. and 1-in. DT specimens are tested on pendulum machines with capacities of 2000 ft-lb and 10,000 ft-lb respectively (Fig. 3), and the absorbed energy is determined from the potential energy associated with the pendulum position(s) after fracture. The 3-in. DT specimen is fractured on a drop-weight machine of 80,000 ft-lb capacity, and the larger 6-in. and 12-in. specimens require a drop-weight machine of 800,000 ft-lb capacity (Fig. 4). In all cases the specimen impact velocities ranged from 25 to 35 ft/sec.

The specimen energy absorbed with the drop-weight machines is determined from the load-versus-time output from the strain gages on the hammer according to the equation

$$\Delta E = I \left(V_0 - \frac{I}{2m} \right), \quad (1)$$

where ΔE is the absorbed energy (ft-lb), V_0 is the hammer impact velocity (ft/sec), m is the mass of the hammer (lb-sec²/ft), and I is the impulse determined from the area under the force-vs-time oscilloscope trace (lb-sec). The relation of the hammer strain-gage output to the specimen force is determined from a static hammer calibration using a hydraulic press. An alternate means of determining the residual energy after fracture is to measure the deflections of soft lead bricks used to absorb the residual hammer energy after the specimen has been fractured. A reproducible lead brick calibration curve has been obtained by dropping the hammer from various heights on the lead bricks with the test specimen removed.

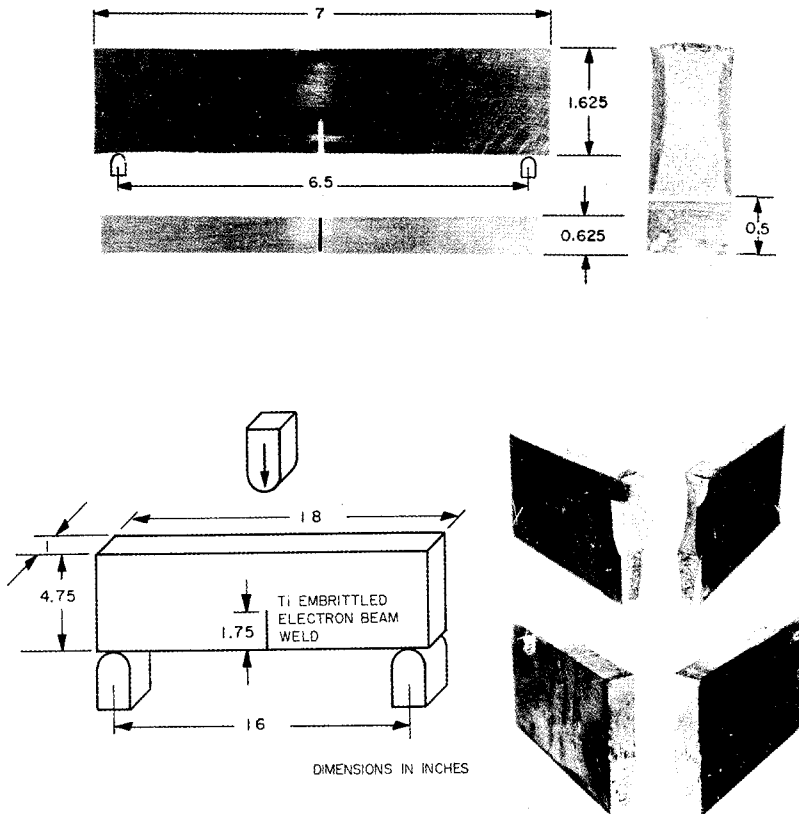
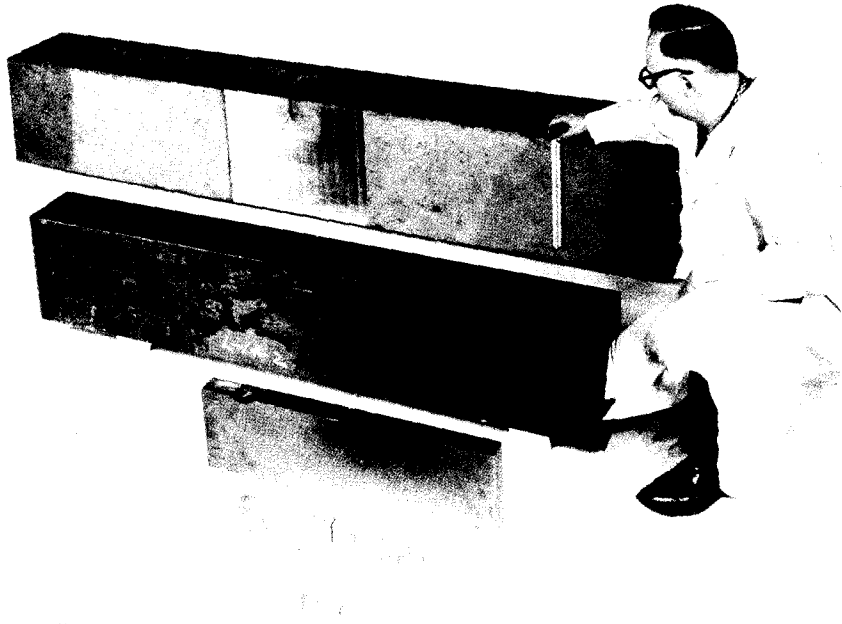


Fig. 1 - Features of 5/8-in. and 1-in. DT specimens. The 5/8-in. DT specimen (top) is illustrated with a machined-notch crack starter having a knife-edge sharpened notch tip. The 1-in. DT specimen (bottom) contains a brittle electron-beam (EB) weld. Either of the two crack starters is used for 5/8-in. DT specimens, but only the EB welds are used for larger DT specimens. The broken halves of the 1-in. DT specimens illustrate brittle and ductile fractures.



70296

Fig. 2 - Various DT specimens used for size-effect studies ranging in thickness from 5/8 in. to 12 in.

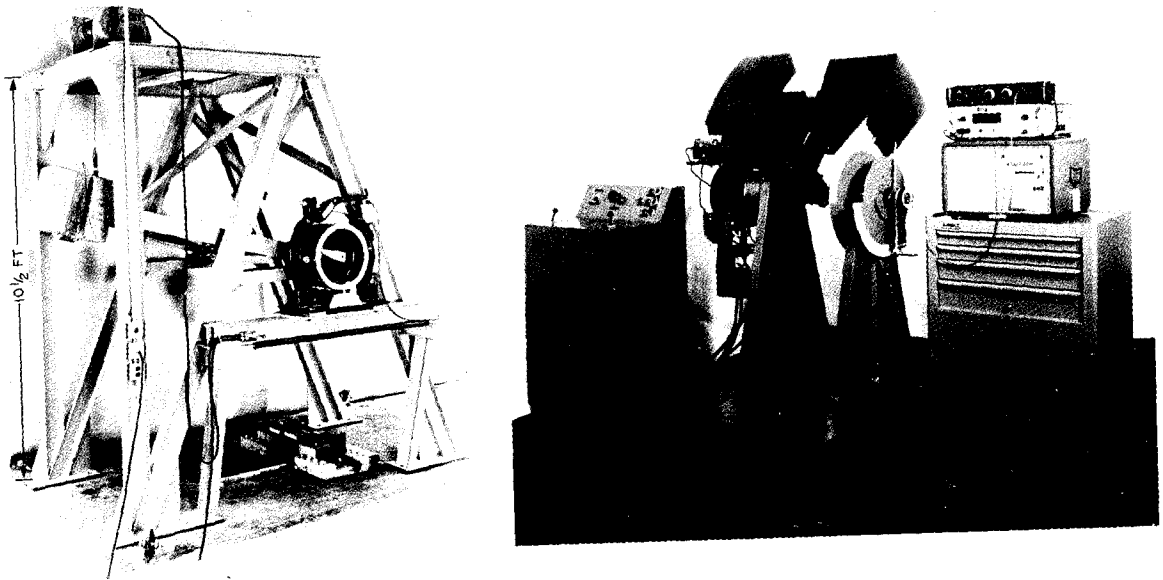


Fig. 3 - DT test pendulum machines. The single-pendulum type (10,000-ft-lb capacity) is on the left. The instrumented, double-pendulum type on the right provides for shockless testing of 5/8-in. DT specimens (2000-ft-lb capacity).

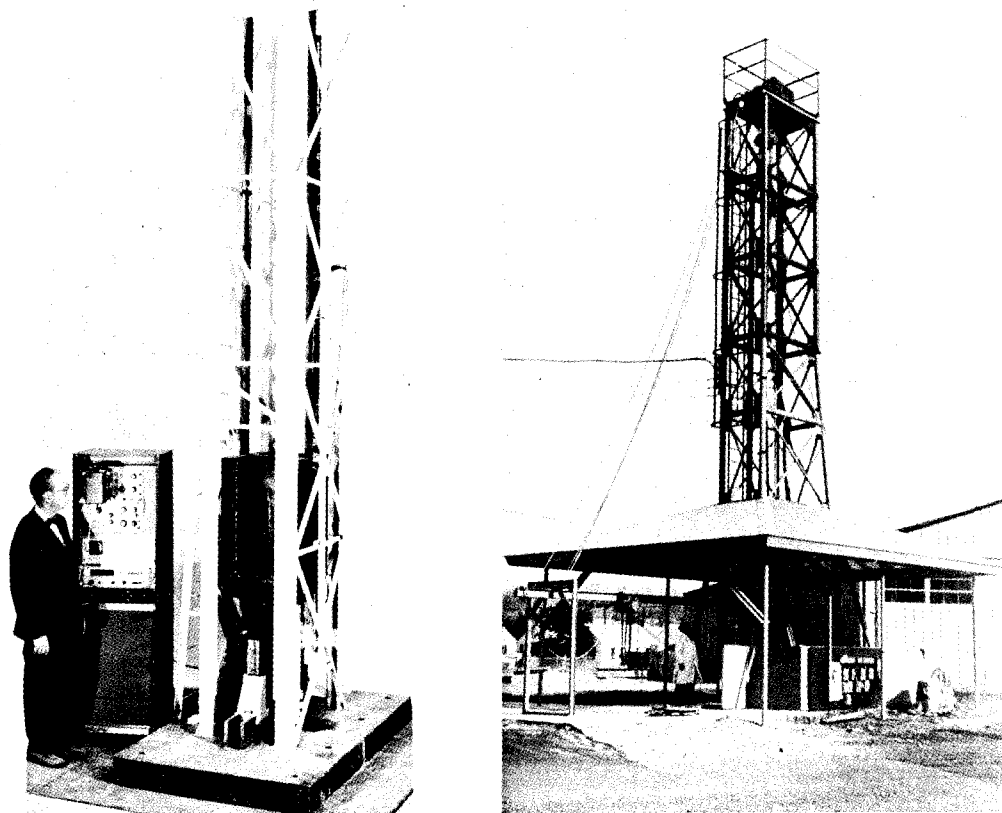


Fig. 4 - Drop-weight type DT machines with capacities of 80,000 ft-lb (left) and 800,000 ft-lb (right)

Table 1
Dimensions and Weights of Various Steel Specimens Used in the DT Test

Specimen Designation	Thickness, B		Depth, W		Length, L		Span Between Supports, S		Brittle Weld or Notch Depth, A		Weight	
	In.	Cm	In.	Cm	In.	Cm	In.	Cm	In.	Cm	Lb	Kg
5/8-in. DT*	0.625	1.6	1.62	4.1	7	18	6.5	16.5	0.5	1.3	2	0.9
1-in. DT	1	2.5	4.75	12.0	18	46	16	40.6	1.75	4.4	24	10
2-in. DT	2	5.0	8	20.3	28	71	26	66.0	3	7.6	127	57
3-in. DT	3	7.6	8	20.3	28	71	26	66.0	3	7.6	190	86
6-in. DT	6	15.2	12	30.5	62	158	58	147.3	3	7.6	1220	554
10-in. DT	10	25.4	15	38.1	90	228	68	172.5	4.5	11.4	3820	1735
12-in. DT	12	30.5	15	38.1	90	228	84	213.3	3	7.6	4580	2080

*The crack starter is either a deep machined notch with tip sharpened by pressed knife edge or a brittle electron beam weld. For the larger specimens, only the brittle weld is used as the crack starter.

The energy recorded includes certain parasitic losses in addition to the energy attributable to the fracture. These include the specimen rotational energy, brinelling of the hammer and anvil into the specimen, and the energy associated with the brittle EB weld. For brittle materials (low-temperature tests) it is known that the fracture energy is a small fraction of the total energy absorbed. For example, a brittle 5/8-in. DT specimen was determined to have a total energy absorption of 50 ft-lb. This specimen was taped back together and the energy recorded upon re-impact was 30 ft-lb. As the energy absorption increases in going through the transition temperature region, the fracture must absorb a greater part of the total energy since the parasitic losses remain essentially constant. This is evident from small changes in the extent of the hammer-brinelled region from a low to a high value of total energy. Also, the specimen rotational energy must, by necessity, decrease when the hammer velocity is reduced further by the fracture of a tough specimen. Tests up to 450° F (232°C) on EB-weld material have indicated that the energy absorbed by the weld is very small and that it exhibits no transition temperature increase. The total change in energy absorbed by the fracture in going through the transition region is typically greater than an order of magnitude. Therefore, it is reasonable to consider the energy associated with a brittle specimen at the low-temperature end of the transition as an effective zero energy. The order-of-magnitude energy increase through the transition temperature region must be attributable primarily to the fracture processes themselves and not to parasitic losses.

The DT test features all of the elements required to impose the maximum-severity mechanical conditions that could occur during structural operation. The typical DT energy curve for a transition temperature steel (Fig. 5) is considered to define a limiting transition temperature region (LTTR) for the thickness in question that is related to a change in the nature of the dynamic fracture propagation from unstable (brittle) to stable (ductile) modes (3).

The beginning of the energy rise is invariably indexed to the drop-weight-test NDT temperature, because this temperature indicates the beginning of a rapid increase in microfracture ductility for the case of dynamic loading (4). The slope or extent of the energy rise at temperatures above NDT may be expected to change with thickness, and this was a subject of the current research reported herein. The NDT point, however, remains fixed for any thickness. This fact is fully described in Ref. 3.

For transition-temperature steels of A533-B quality the transition from brittle to ductile conditions takes place over a relatively narrow temperature interval. The FTE point is defined as the temperature corresponding to the midpoint (50%) of the total energy range. For a steep rise, little variation in FTE temperature will result if a factor different from 50% is used. Since the initial rising portion of the DT curve corresponds to the Robertson CAT curve region, the FTE relates to the CAT at yield stress loading. This was the case for the steel illustrated in Fig. 5 (3).

The full DT curve defines three toughness regimes. Regime 1 is associated with temperatures near NDT, where it is known that small flaws can result in the initiation of catastrophic failure under dynamic loading conditions. This regime corresponds to dynamic LEFM conditions. Regime 3 is associated with a high degree of plastic deformation for which unstable fracture is impossible except by overload or buckling-type conditions. Regime 2 corresponds to the temperature interval between the other two regimes and relates to a transitional phase which is no longer linear elastic nor of the high plastic strain type associated with regime 3. These three regimes are defined by dividing the DT energy curve into thirds (energywise). The applications of these definitions to thick-section A533-B steel was a principal objective of the present research.

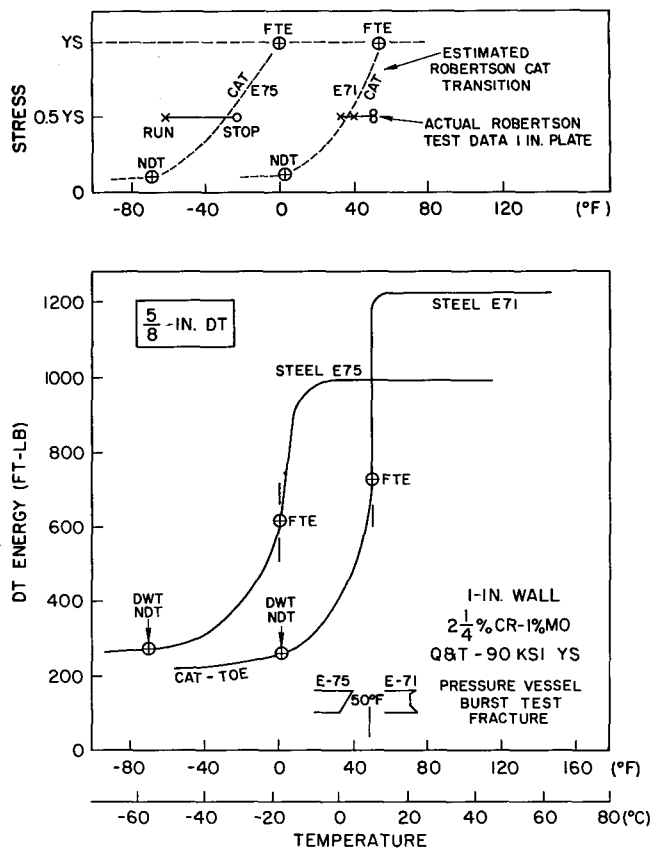


Fig. 5 - Typical shape of dynamic tear (DT) curves for a transition material of high shelf toughness (bottom). The DT energy midpoint indexes the fracture transition—elastic (FTE) temperature, which is equivalent to the crack-arrest temperature (CAT) for yield stress loading (top). The CAT toe region (rise from lower shelf) is indexed to the nil ductility transition (NDT) temperature.

MATERIAL PROPERTIES

The DT studies were conducted on several plates and weldments of A533-B steel. Material was obtained from three 12-in.-thick plates of A533-B Class 1 steel from the HSST Program (HSST plates 01, 02, and 03). The mechanical properties of these plates are listed in HSST progress reports (5,6). A separate 6-in.-thick plate of A533-B Class 2 material was purchased by NRL for investigations of thick-section fracture performance and for irradiation studies. The plate is representative of mill practice in that it is part of a production melt conforming to steel making and rolling practices that are identical with those used in supplying the reactor vessel construction programs. The chemical analysis, mechanical properties, and heat treatment of this plate are summarized in Tables 2a through 2d.

Table 2a
Chemical Analysis for 6-in. A533-B Class 2 Steel

Element	Content (wt-%)	Element	Content (wt-%)
C	0.23	Si	0.20
Mn	1.18	Ni	0.57
P	0.007	Mo	0.46
S	0.014		

Table 2b
Tensile Properties of 6-in. A533-B Class 2 Steel

Location	YS (ksi)	UTS (ksi)	Elongation (%)	RA (%)
Longitudinal				
Surface	79.3	99.2	23.8	66.6
1/2 T	74.1	93.2	25.2	64.5
Transverse				
Surface	83.8	108.8	21.7	60.1
1/2 T	78.9	97.4	23.7	59.6

Table 2c
Charpy-V Data for 6-in. A533-B Class 2 Steel

Temperature		Charpy-V Values* (ft-lb)	
°C	°F	Longitudinal (RW)	Transverse (WR)
-84	-120	13	10
-62	-80	25	18
-40	-40	43	28
-18	0	68	40
4	40	94	55
27	80	108	70
49	120	112	78
71	160	112	78

*Charpy-V energy at NDT (average for 1/4 T and 1/2 T locations equal to +10°F (-12°C)): RW = 75 ft-lb and WR = 43 ft-lb. Fracture appearance transition temperature, FATT (50% shear): RW = -15°F (-26°C) and WR = 0°F (-18°C).

Table 2d
Heat Treatment of 6-in. A533-B Class 2 Steel

Temperature	Time (hr)	Treatment
1670 to 1685°F (910 to 919°C)	6-1/2	Water dip quench
1650 to 1660°F (899 to 904°C)	6-1/2	Water dip quench
1115 to 1125°F (602 to 607°C)	6-1/2	Air cool

A 12-in.-thick submerged arc weld and a 6-in.-thick electroslag weld were also included in the DT investigations. The submerged arc weld (HSST weldment 50) was formed by joining two sections of HSST plate 01. The welding parameters are given in Table 3; additional mechanical properties data are listed in Ref. 7. The electroslag weld (HSST weldment 53) was obtained commercially, and welding data are given in Ref. 8

Table 3
Welding Parameters for 12-in.-Thick A533 Submerged Arc Weld (HSST Weld 50)

Parameter	Root	Remainder
Electrode size and type	1/4 in., E-8018, C-3	3/16 in. B-4 Mod.
Flux type and size	—	Linde 1092, 65-200
Current and polarity (amperes)	325 to 375 dc-SP	650 ac
Arc voltage (volts)	25	31
Travel speed (in./min)	—	13
Welding position	Flat	
Preheat	250° F (121° C), held until postweld heat treatment	
Interpass	500° F (260° C)	
Postweld heat treatment	1150° F ± 25° F (621° C ± 14° C), held 1 hr/in.	
Intermediate postweld heat treatment	1100° F ± 25° F (593° C ± 14° C), held 15 min.	

The DWT NDT for HSST plates 01, 02, and 03 is fairly uniform through the thickness and averaged 10° F (-12° C) with a scatter of approximately ±10° F (±6° C). The plates displayed a shallow surface layer (< 1-1/2 in.) for which the NDT temperature decreased by approximately 100° F (55° C) (5,6). Shallow surface layers of increased toughness were also features of the 6-in. Class 2 plate. The NDT of these layers was approximately -40° F (-40° C).

A comparison of the Charpy-V (C_v) values from the 6-in. Class 2 plate with those from a 12-in. Class 1 plate (HSST 01) is presented in Fig. 6. Both plates indicate a lowering of the upper shelf energy for WR (weak, transverse to the primary rolling direction) specimens in comparison with RW (strong, parallel to the primary rolling direction) specimens. Figure 6 indicates that the conventional 30-ft-lb C_v fix to determine NDT for the normalized A302-B steels is applicable for the 12-in. A533-B Class 1 steel. However, for the 6-in. Class 2 material the figure indicates that a higher fix energy must be employed. In addition, different fix energies apply for RW and WR orientations. The problem of variable C_v energy indexing with changes of steel composition, heat treatment, and strength levels becomes apparent in these comparisons.

THROUGH-THICKNESS FRACTURE TOUGHNESS VARIATIONS FOR PLATES AND WELDMENTS

12-in. A533-B Class 1 Plates

The 5/8-in. DT specimen was used to characterize the toughness variation through the thickness of three 12-in.-thick plates of A533-B Class 1 steel (HSST plates 01, 02, 03). The test material represents a sampling of one location in all three plates. Specimens were taken from thickness locations symmetrical about the midthickness plane in order to define any asymmetrical variations resulting primarily from nonuniform rates of heat removal during quenching (HSST plates 01 and 02 were quenched in the vertical position, and plate 03 was quenched horizontally). Most specimens were cut in the RW

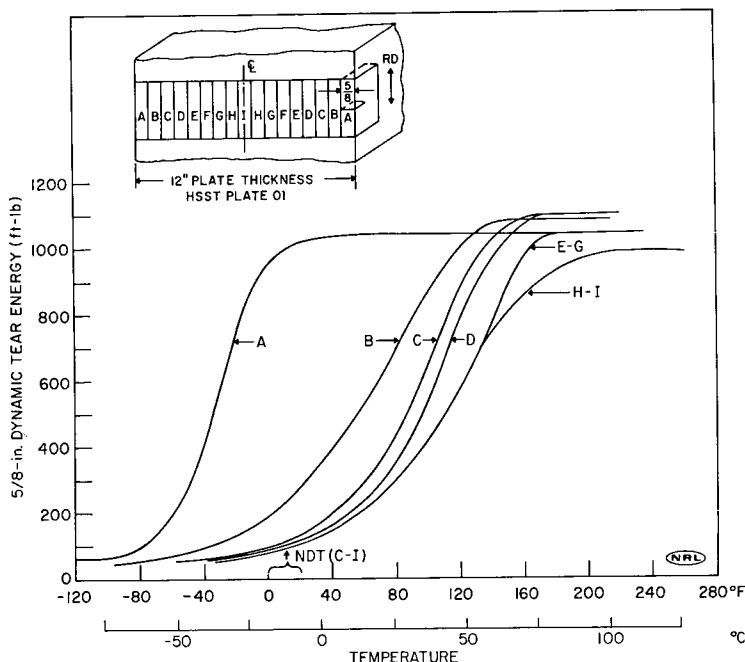


Fig. 7 - Variation in fracture toughness through the thickness of a 12-in. A533-B Class 1 steel (HSST plate 01), determined by 5/8-in. DT specimens in the RW (longitudinal) orientation. The curves are drawn as a best fit through the data.

The data points in Fig. 7 (more than 150) are omitted for the sake of clarity. To illustrate the degree of scatter the individual data points of curve H-I (Fig. 7 and Table A1) are shown in Fig. 8. The results of specimens having two different notch preparations (EB or machined notch with pressed tip) are illustrated in Fig. 8. No trend in the data can be attributed to the method of notch preparation. A comparison of the fracture surfaces for specimens from locations F and G having both types of crack starter is shown in Fig. 9. In addition to the fracture energies, the transition in fracture appearance from cleavage to dimpled rupture is similar for both types of specimens.

A similar through-thickness survey of the RW toughness variation was conducted for HSST plate 02. As for HSST plate 01 the best fit curve is drawn through the data points at a given thickness location (Fig. 10 and the portion of Table A2 for the RW orientation). A comparison of Figs. 7 and 10 indicates that plates 01 and 02 display nearly identical trends in fracture toughness. Both plates reach approximately the same shelf level toughness, have a tough surface layer less than 1-1/2-in. deep, and exhibit no asymmetrical variations about the midthickness plane. The transition region for plate 02 evolves about 10°F (6°) lower than that for plate 01, and it does not show the slight shelf degradation in toughness at the midthickness locations (H-I) that was displayed by plate 01.

A limited investigation of the DT toughness variations in also the WR orientation through the thickness of HSST plate 02 was conducted with the 5/8-in. DT specimen. The results for the surface, 1/4 T, and 1/2 T are shown in Fig. 11 (and Table A2), where a comparison is made with the RW results at similar thickness locations. The transition regions for both orientations are identical; this result is consistent with the general behavior of ferritic steels. The shelf toughness in the WR orientation is approximately 75% of the RW level for all locations through the thickness; this result is also consistent with trends displayed by other steels in this category.

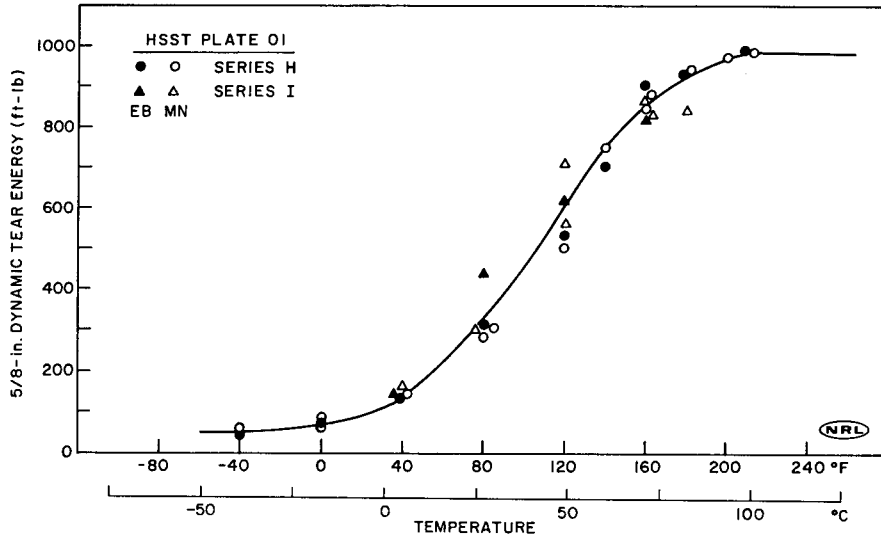


Fig. 8 - Example of the scatter in Fig. 7. Shown here are the 5/8-in. DT data for locations H and I. The specimens have both types of crack starter: an electron-beam weld (EB) and a machined notch with a pressed tip (PN).

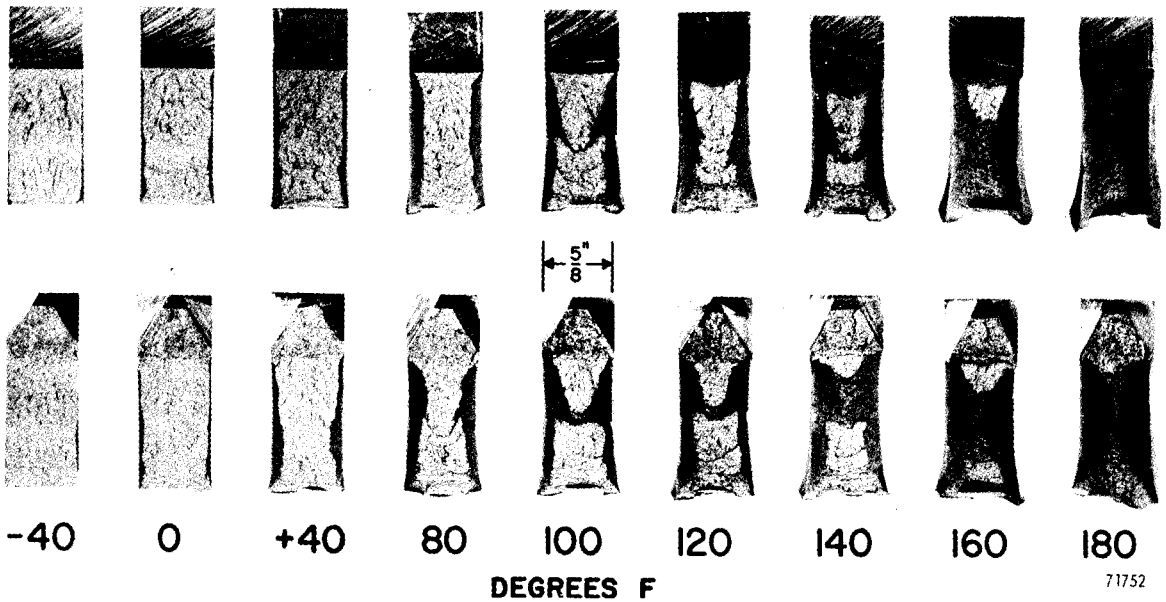


Fig. 9 - A comparison between fracture surfaces of specimens with the electron-beam-weld crack starters (lower row) and specimens with the machined-notch crack starters (upper row). These 5/8-in. DT specimens are from locations F and G (Fig. 7) of A533-B Class 1 steel (HSST plate 01) and are in the RW orientation.

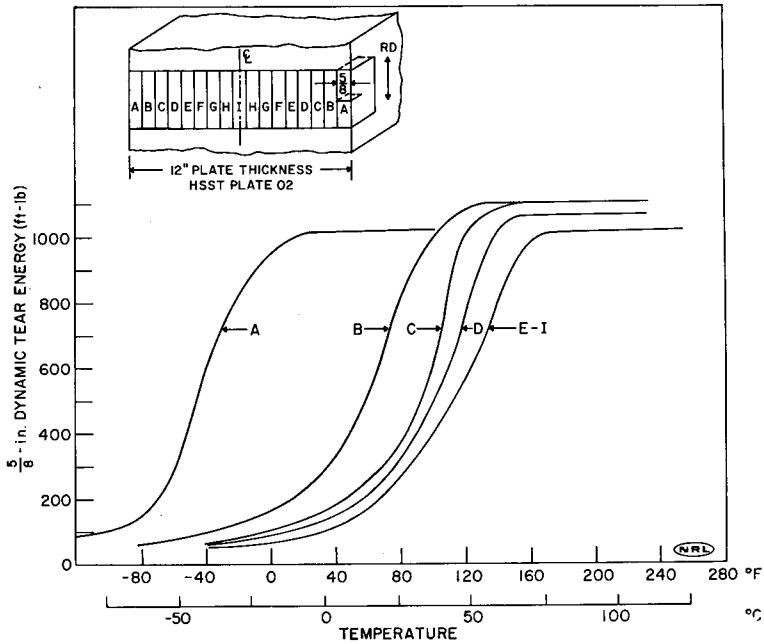


Fig. 10 - Variations of fracture toughness through the thickness of a 12-in. A533-B Class 1 steel (HSST plate 02), determined by 5/8-in DT specimens in the RW orientation

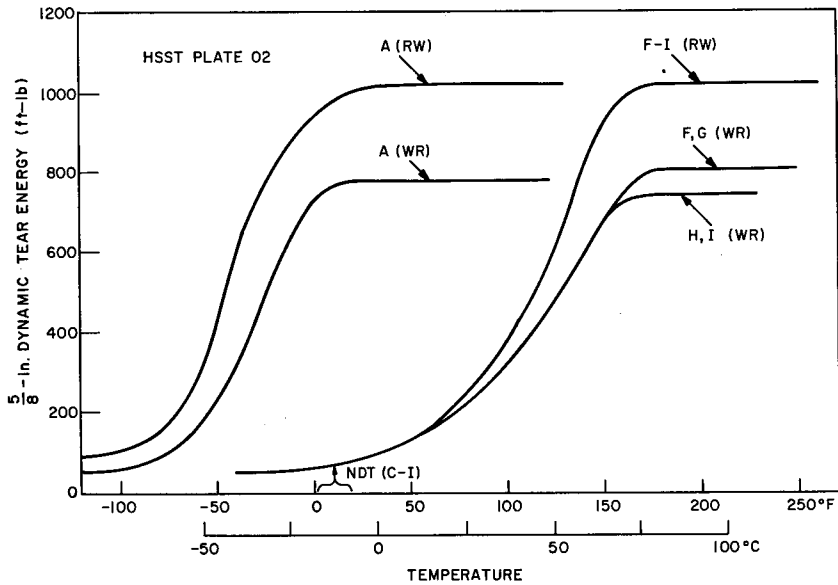


Fig. 11 - A comparison of the toughness variations in RW and WR orientations at specific locations through the thickness of a 12-in. A533-B Class 1 steel (HSST plate 02). The 5/8-in. DT specimen locations with respect to thickness are as specified in Fig. 10.

The results of a 5/8-in. DT through-thickness survey for HSST plate 03 is shown in Fig. 12 (and Table A3). The toughness variations are similar to those displayed for HSST plates 01 and 02, including a tough surface layer and uniform shelf-level toughness throughout the thickness. A comparison of the toughness trends of HSST plate 03 with those of plate 02 is presented in Fig. 13, where it is seen that plate 02 displays a slightly better toughness at a given temperature in the transition region. Since plate 03 was quenched in the horizontal position, it was expected that any asymmetrical variations in toughness about the midthickness would most likely be evident near the surface, where the temperature gradient during quenching is greatest. Figure 14 illustrates the individual energy values from specimens taken from symmetrical locations about the 1/2 T plane near the surface. There is no evidence of an asymmetrical behavior for these locations (layer A) nor for the material closer to the midthickness.

Toughness to 600°F (316°C)

A 5/8-in. DT investigation of the fracture toughness at elevated temperatures was conducted on material from HSST plate 01 in the RW orientation (layer D in Fig. 7). The results (Fig. 15 and Tables A1 and A4) indicate that the shelf-level energy remains essentially constant at least up to 600°F (316°C). The toughness eventually must drop off

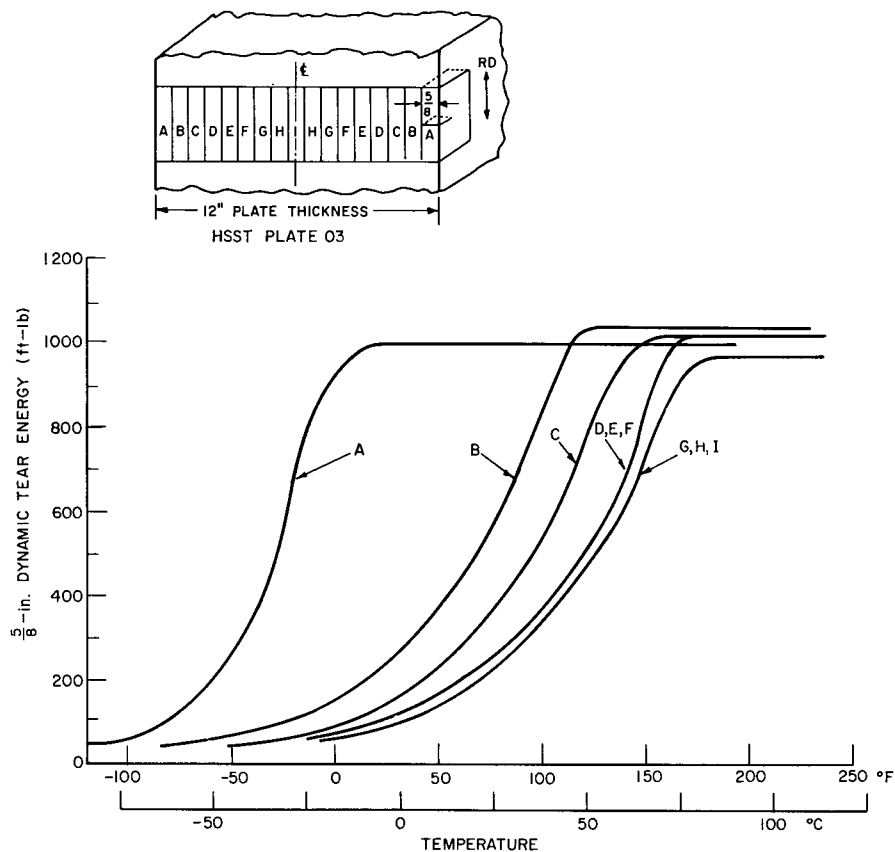


Fig. 12 - Variations in fracture toughness through the thickness of a 12-in. A533-B Class 1 steel (HSST plate 03), determined by 5/8-in. DT specimens in the RW orientation with machined-notch crack starters

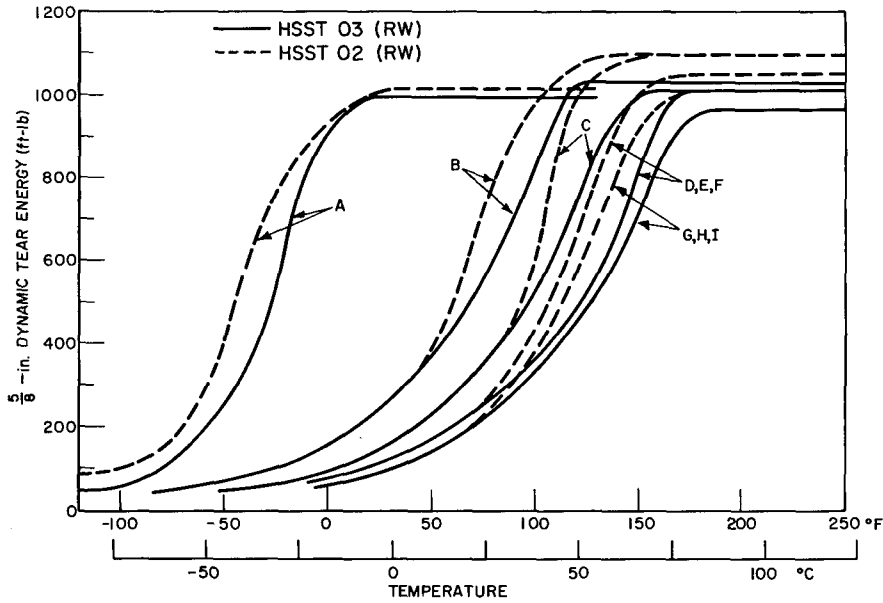


Fig. 13 - A comparison of the toughness variations through the thickness of the two 12-in. A533-B Class 1 plates shown in Figs. 10 and 12 (HSST plates 02 and 03)

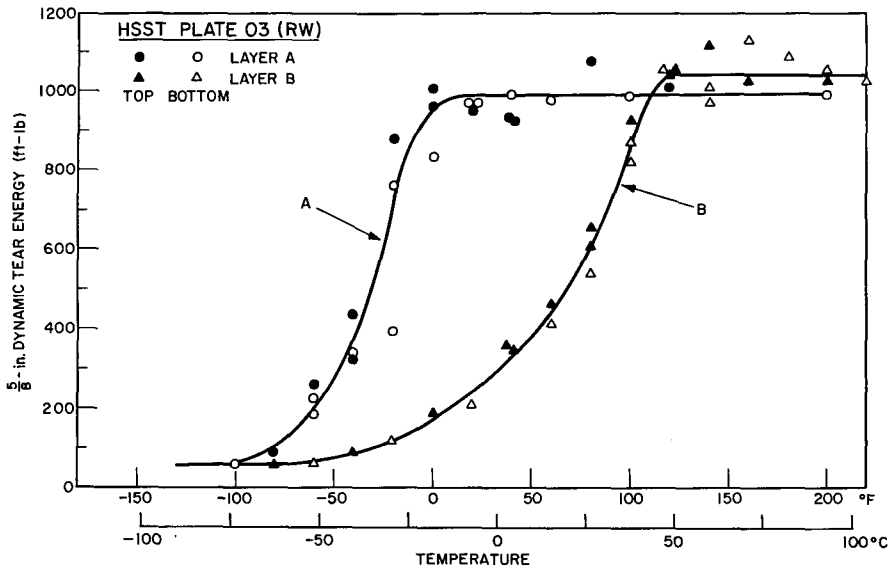


Fig. 14 - Example of the variation in the 5/8-in. DT data for thickness locations A and B (Fig. 12) of a 12-in. A533-B Class 1 steel (HSST plate 03). The data indicate no trend between plate material from the top and bottom surfaces (right and left as sketched in Fig. 12) as a result of the plate being quenched in the horizontal position.

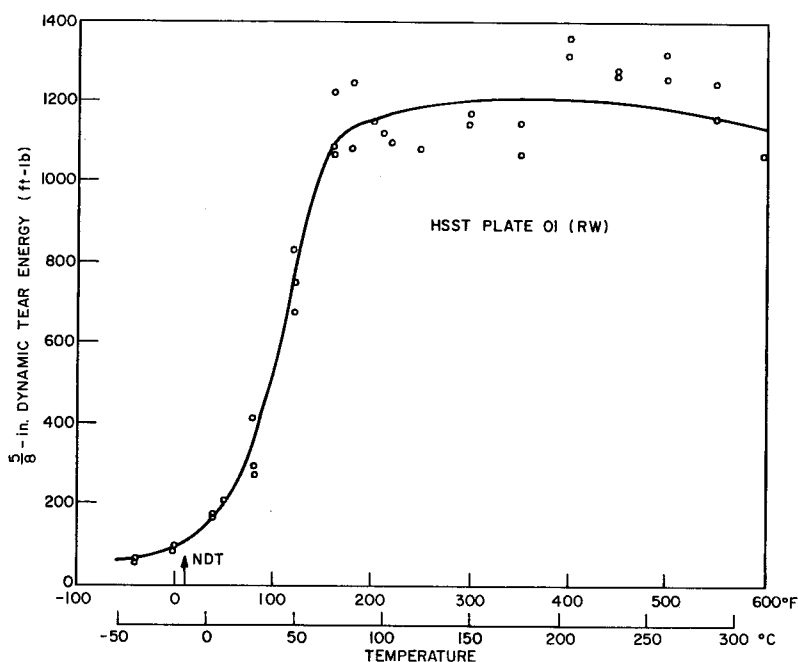


Fig. 15 - Elevated temperature fracture toughness of a 12-in. A533-B Class 1 steel (HSST plate 01) as determined with 5/8-in. DT specimens taken from layer D (Fig. 7). The specimens were in the RW orientation.

at higher temperatures, but this would appear to be above the region of interest for nuclear pressure vessels. This investigation justifies the practice of not obtaining data for 5/8-in. specimens beyond the temperature where the upper shelf is attained. For A533-B steel this temperature invariably correlates with the lowest temperature at which all cleavage is eliminated, as visible to the naked eye.

6-in. A533-B Class 2 Plate

A 5/8-in. through-thickness survey similar to that for HSST plates 01, 02, and 03 was conducted for a 6-in. A533-B Class 2 plate which was not part of the HSST Program. The results of RW specimens from two plate locations 5 ft apart are shown in Fig. 16 (and Table A5). The specimens cut from the surface layer (location A) are not plotted because of the scatter (Table A5 listing the individual values). The solid lines represent the best fit through the data points from the other four symmetrical thickness locations (B, C, D, and E) about the 1/2 T plane. Specimens having both EB and machined-notch crack starters are included, and no trends due to notch preparation are evident. A symmetrical trend, similar to HSST plates 01, 02, and 03, was displayed for thickness locations about the 1/2 T plane. The scatter band for locations B through E is shown in the figure; this scatter band is somewhat greater than that displayed by the three HSST plates. Most of the values from the surface specimens fall within the scatter band in the transition region, and all specimens are included in the scatter band at the shelf-level temperatures, above 150°F (66°C). A tough surface layer is indicated, but its thickness is probably less than 1/2 in. The data indicate similar trends in the transition region for locations B through E, but a progressive lowering of shelf toughness is evident with thickness locations toward the 1/2 T plane. The midthickness exhibits an average lowering of DT shelf energy amounting to about 20% of the value of layer B.

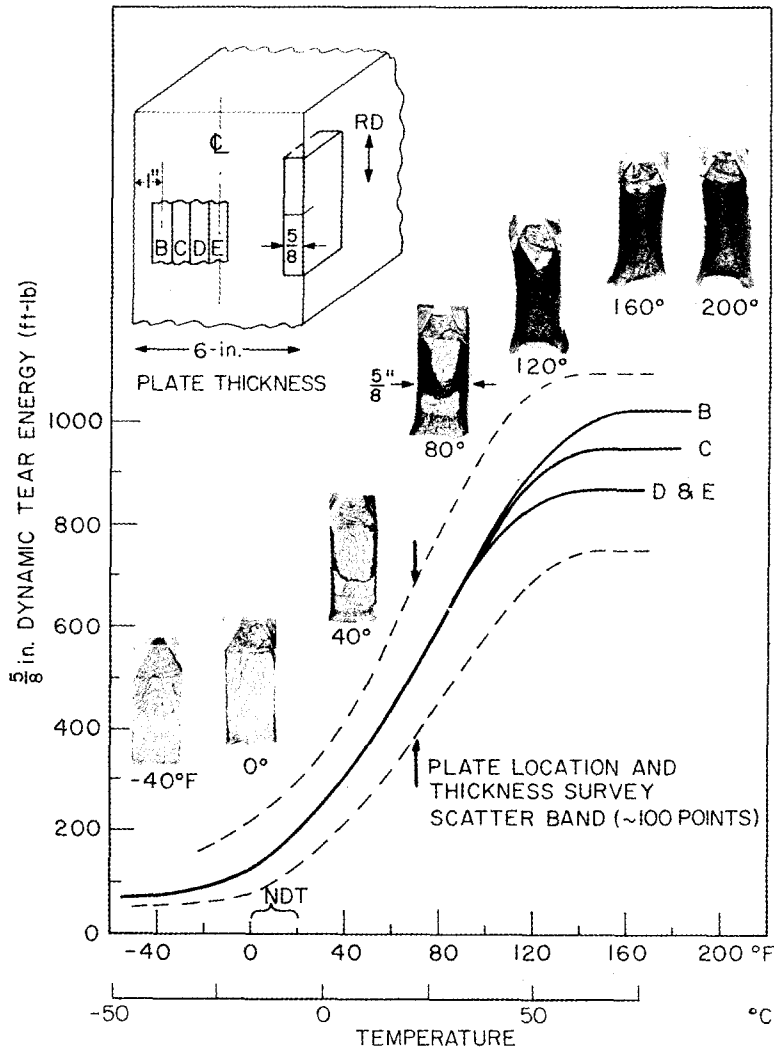


Fig. 16 - Variations in fracture toughness through the thickness of a 6-in. A533-B Class 2 plate, determined by 5/8-in. DT specimens in the RW orientation. The fracture surfaces at selected temperatures are illustrated.

A comparison of the 5/8-in. DT trends (RW) of this plate with HSST 01 is presented in Fig. 17. Generally with locations toward the midthickness plane the transition temperature region for the 6-in. plate evolves approximately 40°F (22°C) lower in temperature than does that for HSST plate 01. However, the spread in shelf-level energies for the 6-in. plate is greater than for HSST plate 01.

A study of 5/8-in. DT specimens in the WR orientation was completed for locations C and E shown in Fig. 16. The comparison of the RW and WR values is presented in Fig. 18 (and Table A5). The results are consistent with those observed in Fig. 11 for HSST plate 02. The transition region for the WR orientation evolves in the same temperature interval as the RW orientation but attains a lower shelf energy. The WR shelf of mid-thickness material is lowered to approximately 75% of the RW shelf; for layer C the drop of the WR shelf is to approximately 70% of the RW shelf.

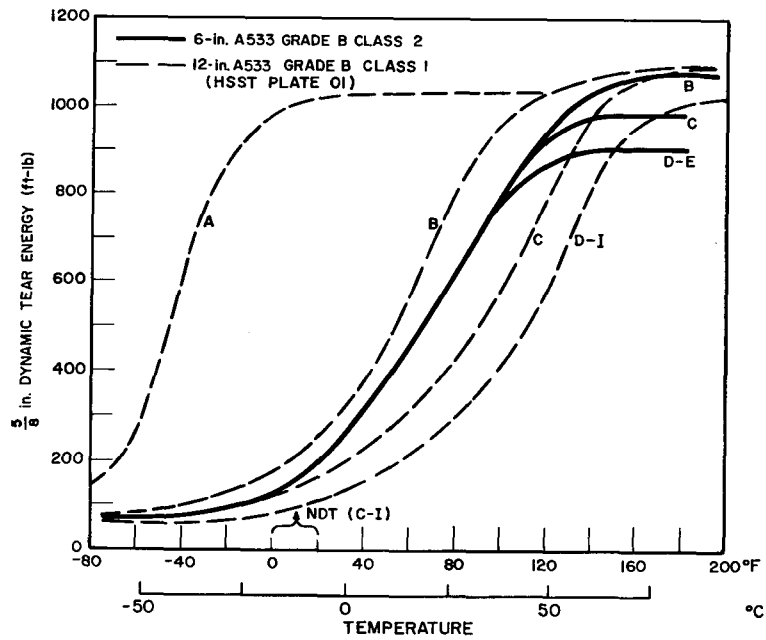


Fig. 17 - A comparison of the toughness variations through the thickness of a 6-in. A533-B Class 2 steel (Fig. 16) and a 12-in. A533-B Class 1 steel (HSST plate 01) (Fig. 7). The letters beside the curves indicate the thickness locations of the 5/8-in. DT specimens in the RW orientation for the plates being compared (Figs. 7 and 16).

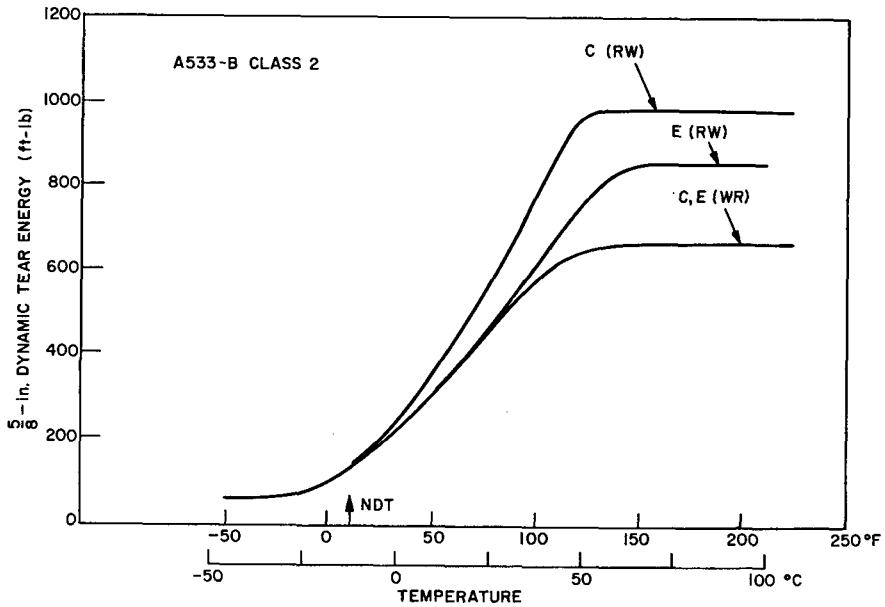


Fig. 18 - A comparison of the toughness variations in the RW and WR orientations at specific locations through the thickness of a 6-in. A533-B Class 2 plate. The 5/8-in. DT specimen locations with respect to thickness are as specified in Fig. 16.

12-in. A533 Submerged Arc Weld

The fracture toughness of a 12-in.-thick A533 submerged arc weld was characterized with the 5/8-in. DT specimens. The weld, HSST weld 50, was formed with HSST plate 01 material. Specimens were cut from the center of the weld in two orientations, as shown in Fig. 19 together with the DT results (Table A6). The DT energy values exhibit considerable scatter, but no trend was noted due to location or orientation. The overall weld performance can be assessed by means of the scatter envelope shown in Fig. 19.

In Fig. 20 the envelope from Fig. 19 is replotted in the framework of the 5/8-in. DT through-thickness survey for HSST plate 01 (Fig. 7). Note that the weld generally exhibits a toughness transition region that is 60°F (33°C) lower in temperature than the plate. The weld metal also attains a higher shelf toughness, indicating that it is of better quality than the plate.

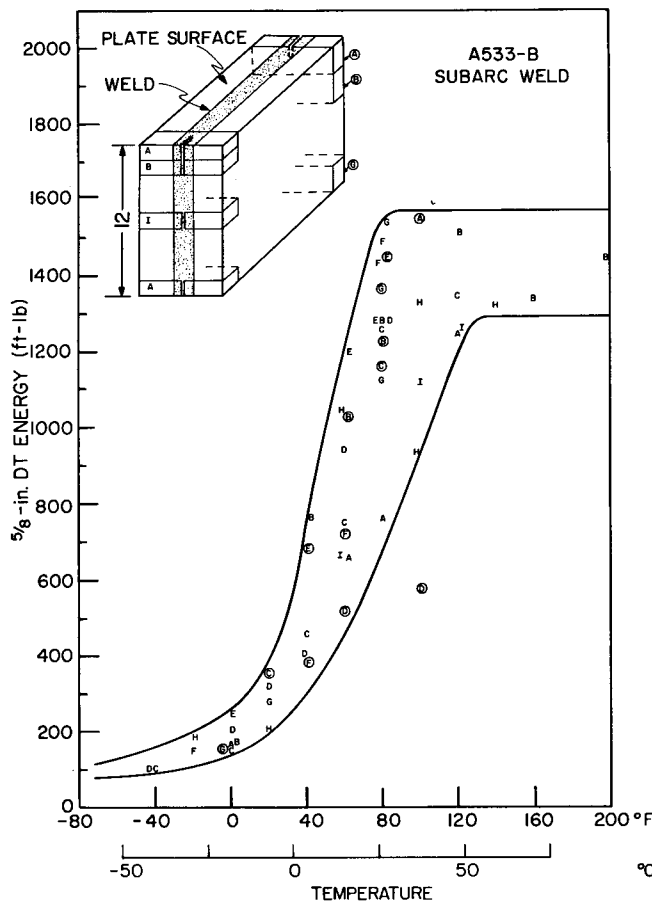


Fig. 19 - Variations in fracture toughness through the thickness of a 12-in. A533 submerged arc weld as determined by 5/8-in. DT specimens with EB-weld crack starters

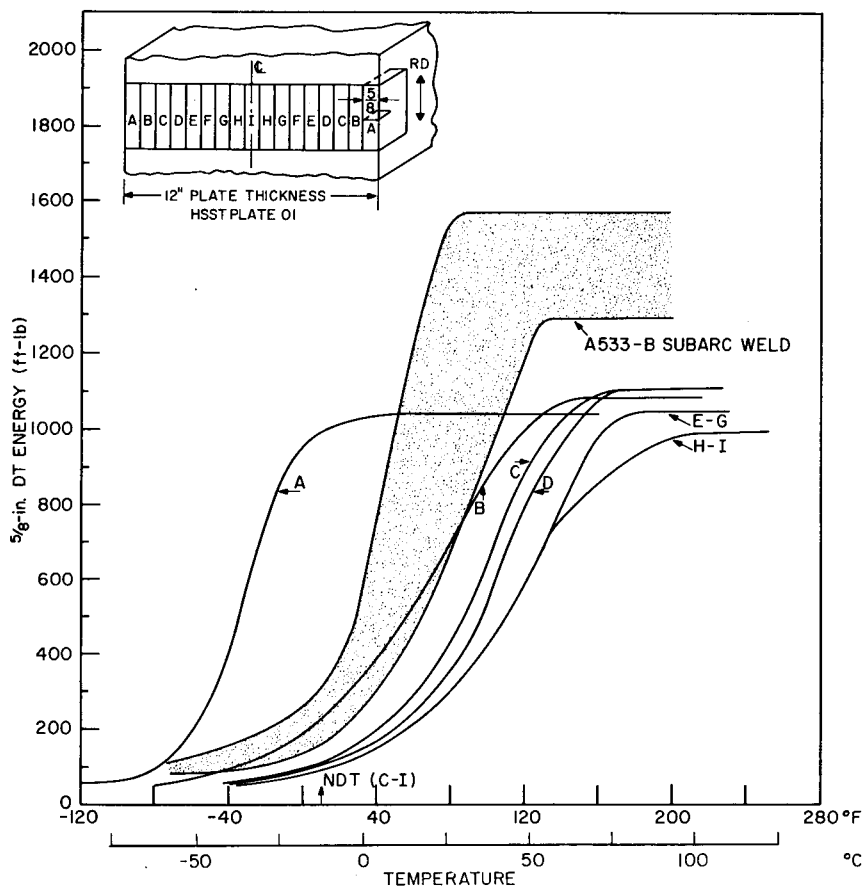
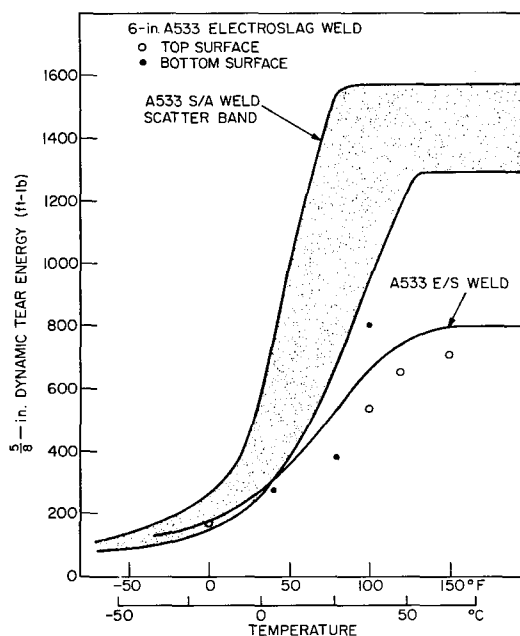


Fig. 20 - Comparison of the fracture toughness exhibited by the A533 submerged arc weld (Fig. 19) with the 5/8-in. DT through-thickness survey (RW orientation) for the plate material (Fig. 7). The weld exhibits a transition behavior generally 60° F (33° C) lower than the plate and also attains a higher shelf level due to improved metallurgical quality.

6-in. A533 Electroslag Weld

A 5/8-in. DT survey was conducted on the surface layer of a 6-in. A533 electroslag weld (HSST weld 53). The specimen orientation is similar to the specimens designed with an uncircled A in Fig. 19. The results are shown in Fig. 21 (and Table A7) along with the scatter band from the A533 submerged arc weld from Fig. 19. The extent of the scatter band from a through-thickness survey for the electroslag weld is not known, and only an approximate curve representing surface material is shown. Insufficient specimens were taken to arrive at definite conclusions concerning the toughness trends throughout the entire electroslag weld. It is clear, however, that the transition regions for both the electroslag and submerged arc welds evolve in the same temperature interval and that the shelf toughness of the electroslag weld is considerably lower than that for the submerged arc weld. Nevertheless the shelf toughness of the electroslag weld is equivalent to that of the WR specimen orientation for both the 6-in. and 12-in. A533-B plates. In addition the transition region for the weld evolves in a lower temperature interval than that for the plates studied.

Fig. 21 - Variation in fracture toughness of the surface material from a 6-in. A533 electroslag (E/S) weld as determined with the 5/8-in. DT specimen. The specimen orientation is identical to that labeled with an uncircled A in Fig. 19. Comparison of this electroslag weld with the submerged arc (S/A) weld illustrated in Fig. 19 shows the electroslag weld to reach a substantially lower shelf toughness, but it is still of the same magnitude as the shelf toughness of a 6-in. A533-B Class 2 plate (Fig. 18) and a 12-in. A533-B Class 1 plate (HSST 02) (Fig. 11) both in the WR orientation.



THICK-SECTION DT STUDIES

The 5/8-in. DT studies described were extended to thicker specimens to ascertain the size effect due primarily to the thickness-induced mechanical constraint. These investigations involved 1-, 3-, and 12-in. DT specimens from a 12-in. A533-B Class 1 plate (HSST 01) and 1-, 3-, and 6-in. DT specimens from a 6-in. A533-B Class 2 plate.

1-in. DT Investigations

Variations in fracture toughness through the thickness of HSST plate 01 were defined by the 1-in. DT specimen (RW). The results from six thickness locations symmetrical to the midthickness plane are presented in Fig. 22 (and Table A8). The results display a brittle-ductile transition behavior which evolves within 160°F (89°C) above NDT. The tough surface layer which was defined as less than 1-1/2 in. deep by the 5/8-in. DT survey is reflected in the performance of the 1-in. DT specimens from the surface layers (layers A and B in Fig. 22). The majority of the plate (layers C through F) is of uniform toughness, with the material from the midthickness plane (layer F) exhibiting a slightly lower shelf toughness. No asymmetrical variations in toughness about the 1/2 T plane were detected.

A higher degree of scatter is exhibited by the shelf-level region as compared to the transition region. The upper region of the shelf scatter band is attributed to crack branching at the base of the EB crack starter weld as illustrated at the upper right in Fig. 22. A similar behavior has been noted for thicker specimens of very high toughness and is a reflection of the tendency to form a large plastic zone as the crack enters the plate material from the brittle crack starter region. The lower values in the upper shelf scatter band (layer F) result from the poorer metallurgical quality near the midthickness location. Even these lower values reflect a high degree of fracture toughness, and extensive through-thickness plastic deformation is required to propagate the fracture.

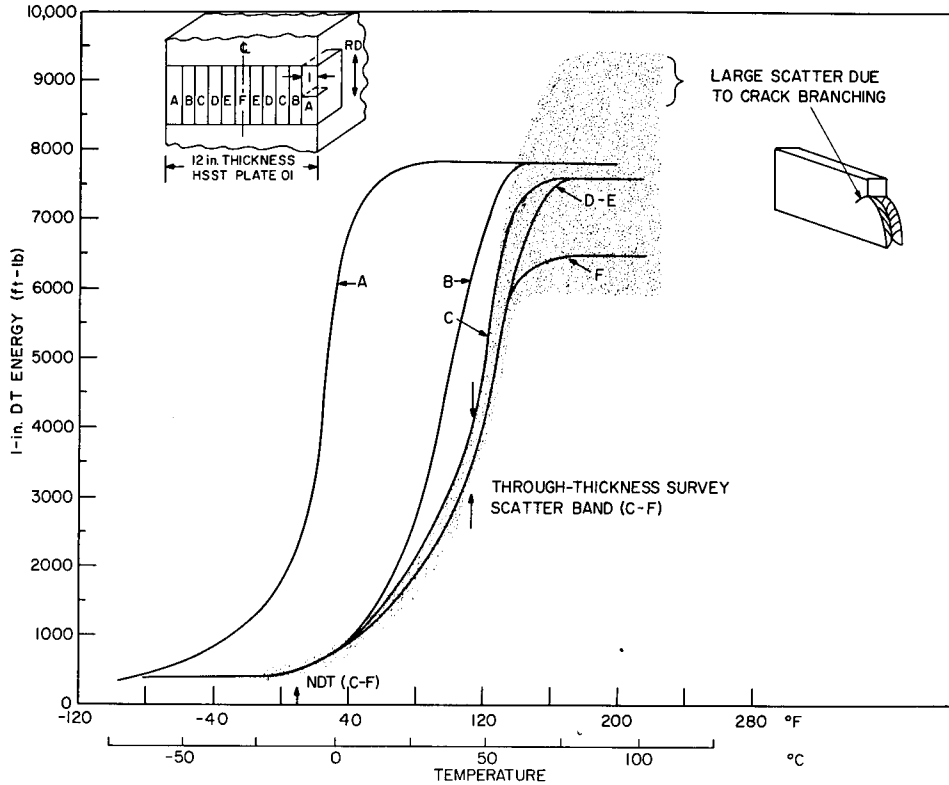


Fig. 22 - Variation of the fracture toughness through the thickness of a 12-in. A533-B Class 1 steel (HSST plate 01) as determined by 1-in. DT specimens in the RW orientation. The high end of the shelf scatter band is attributed to crack branching as the crack enters the test material from the brittle crack-starter region.

A corresponding investigation with 1-in. DT (RW) specimens was conducted for a 6-in. A533-B Class 2 plate. The results are similar to those of the 12-in. A533-B Class 1 plate described above. The data from three locations through the thickness are summarized in Table A9, and the best fit curve for specimens at the 1/2 T location is shown in Fig. 23. In the photographs in Fig. 23 the order-of-magnitude increase in energy absorption throughout the transition temperature region is reflected by a change in the microscopic fracture appearance from cleavage to dimpled rupture.

3-in. DT Investigations

The 3-in. DT specimen represented the largest intermediate thickness investigated. The resulting toughness trends for the 12-in.-thick HSST plate 01 at the surface and 1/2 T locations (RW and WR) are shown in Fig. 24 (and Table A10). As with the 5/8-in. and 1-in. specimens, an order-of-magnitude increase in energy absorption is displayed in the transition temperature interval, which evolves within the 200°F (111°C) interval above NDT. The rate of energy increase, however, is depressed in the lower toe regions as compared to the curves for 5/8- and 1-in. specimens (Figs. 7 and 22).

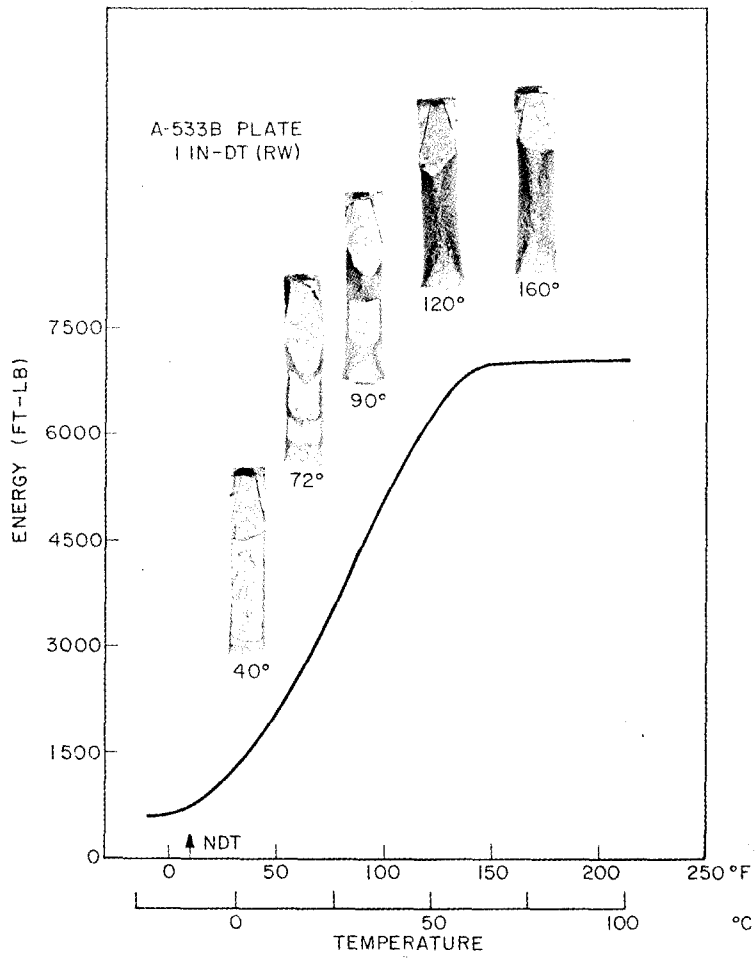


Fig. 23 - Transition temperature behavior of 1-in. DT energy from the midthickness location of a 6-in. A-533-B Class 2 steel. The specimens were in the RW orientation.

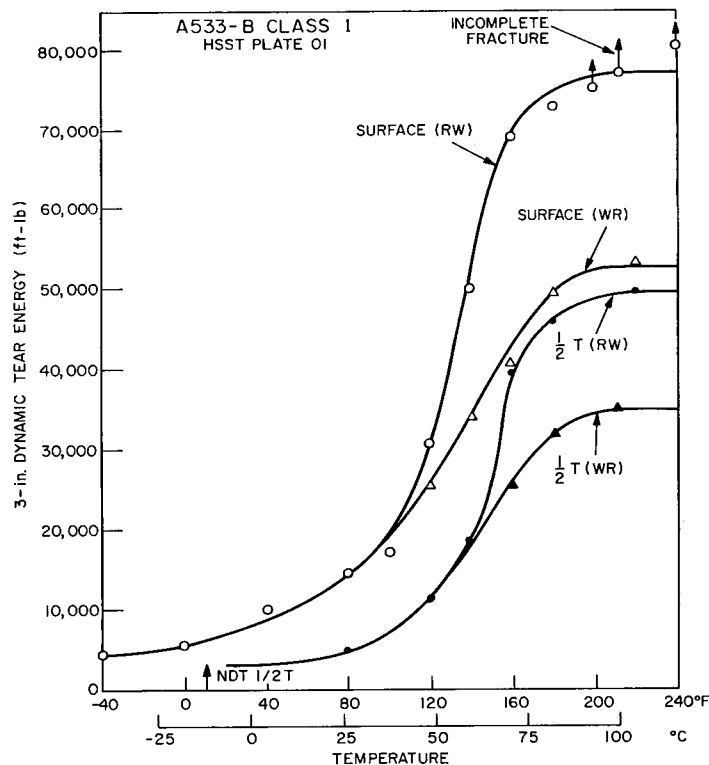


Fig. 24 - 3-in. DT comparison of fracture toughness in the RW and WR orientations for surface and 1/2 T locations for a 12-in. A533-B steel (HSST plate 01)

Figure 24 brings to light several additional features. First, at a given thickness location the drop in shelf level toughness between RW and WR orientations closely resembles that displayed by the 5/8-in. DT results (Fig. 11). The 3-in. DT values in Fig. 24 indicate that the ratio of WR to RW shelf energies for both surface and 1/2 T locations is approximately 0.7 compared to 0.75 for the 5/8-in. DT specimens sketched in Fig. 7. Second, a degradation in shelf-level toughness of midthickness material becomes apparent for both RW and WR orientations (i.e., the ratio of 1/2 T to surface shelf energies for 3-in. DT specimens is 0.65 for both orientations).

This midthickness degradation of toughness is not expected on the basis of the 5/8-in. DT survey, which indicated the plate was of essentially uniform toughness throughout with the exception of a slight lowering at midthickness expressed by a ratio of 1/2 T to surface shelf energy of 0.92 (Fig. 7). This degradation is not as severe as that indicated by the 0.65 ratio for the 3-in. DT specimens. Furthermore the 3-in. DT specimens at the 1/2 T location contain only 60% of the material which exhibits a slight lowering of shelf toughness, that is, three 5/8-in. DT layers. The remaining 40% of the specimen contains material which exhibits no difference in shelf toughness compared to the surface material, based on 5/8-in. DT trends. Consequently, one would predict a ratio of 1/2 T to surface 3-in. DT shelf energy of 0.95 by summing up the individual 5/8-in. DT trends (compared with the 0.65 value actually observed).

Evidently the degradation in 1/2 T shelf toughness in the 3-in. DT specimen is attributable to a thickness effect which magnifies the slight degradation in shelf toughness

determined with the 5/8-in. DT specimens. This conclusion is borne out by the fact that the 1-in. DT specimens exhibit a ratio of 1/2 T to surface (RW) shelf energy of 0.85 (Fig. 22); this ratio is intermediate to the 0.92 and 0.65 ratios for the 5/8-in. and 3-in. DT specimens respectively.

The results of a 3-in. DT survey using specimens in the RW orientation from the 6-in. A533-B Class 2 plate are shown in Fig. 25 (and Table A11) along with the fracture surfaces of selected specimens. Each specimen comprises material from the surface to the midthickness plane, so that a direct comparison of locations with the surface and 1/2 T location for HSST plate 01 is not possible. However, the shelf toughness is approximately equal to the average of the surface and 1/2 T shelf values for the RW orientation for plate 01 (Fig. 24). Note the appearance of a flat fibrous region in the photograph of the 200° F (93° C) specimen shown in Fig. 25. The thinner specimens displayed full slant fracture on the upper shelf; the same was true for the 3-in. DT (RW) shelf specimens from the surface layer of HSST plate 01 but not for other locations (Fig. 24).

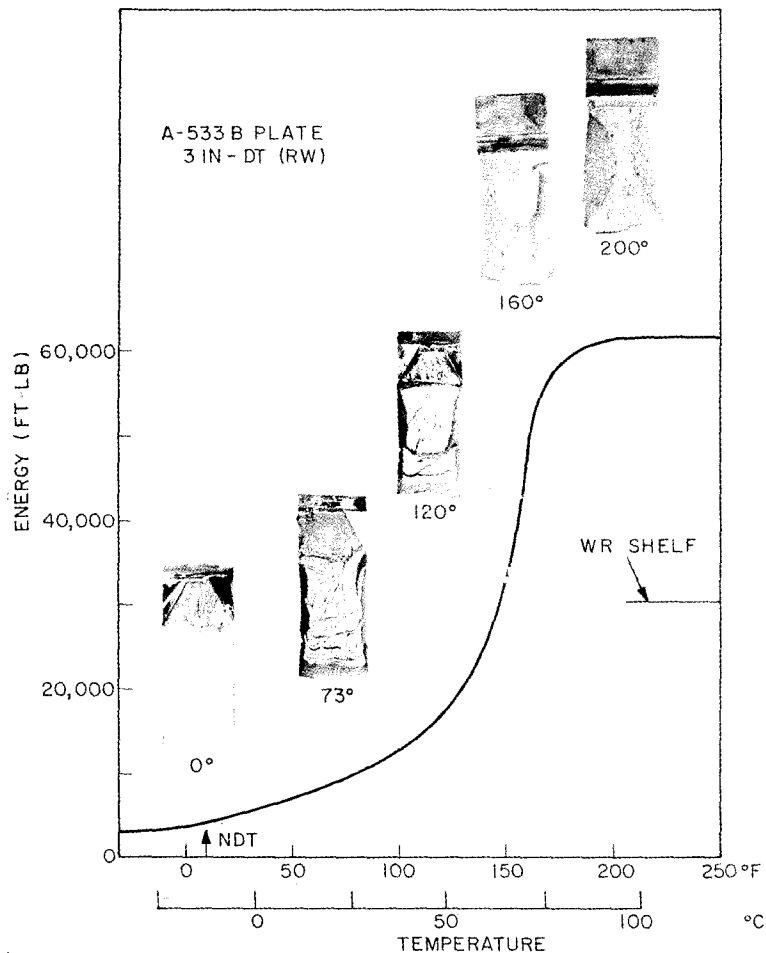
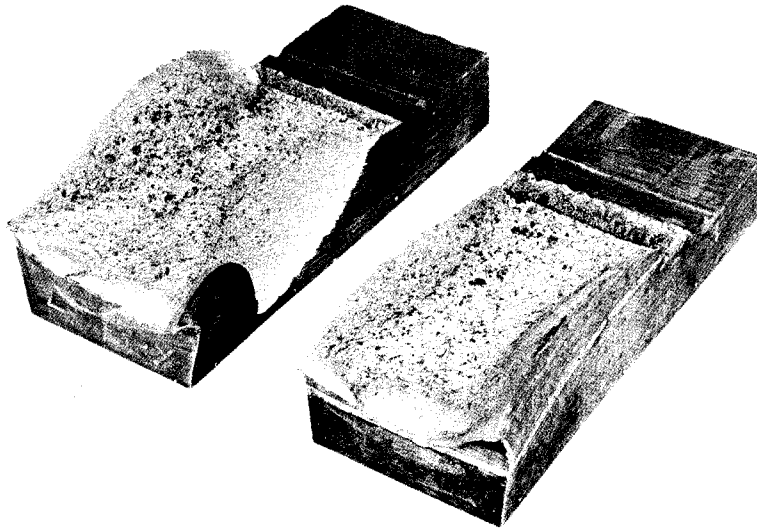


Fig. 25 - 3-in. DT toughness variation of a 6-in. A533-B Class 2 plate. The fracture surfaces and complete curve refer to specimens in the RW orientation. The shelf-level energy of WR specimens is also indicated. All specimens are taken from material spanning the surface to midthickness location.

A complete 3-in. DT survey in the WR orientation for the 6-in. Class 2 plate was not attempted. A spot check of the shelf energy, however, indicated 31,000 ft-lb (Fig. 25). The resultant drop in shelf level toughness from RW to WR orientations is about 50% as compared to 30% for both the surface and the 1/2 T locations for HSST plate 01 (Fig. 24). This drop in shelf-level energy between the RW and the WR orientation for the 6-in. plate is reflected in the fracture appearance (Fig. 26).



73379

Fig. 26 - 3-in. DT upper shelf fracture surfaces from RW (left) and WR (right) orientations of the same plate location described in Fig. 25. The variations in fracture appearance are reflected by the differences in shelf energy (Fig. 25).

To characterize the effect of variable specimen geometry on upper shelf performance, two 3-in.-thick specimens from the 6-in. 533-B Class 2 plate were geometrically scaled to the proportions of the 5/8-in. DT specimen. The dimensions of the two specimens were (see Table 1): B, 3 in.; W, 7.8 in.; L, 33.6 in.; S, 31.2 in.; and a, 2.4 in. The primary change was in the span between anvil supports, which was increased to 31 in. over the normal 26-in. value for a 3-in. DT specimen. A small change was also necessary in the unbroken ligament area. The results (Table A12) indicate no differences in energy/area (E/A) as compared to the 3-in. DT (RW) shelf E/A computed from Fig. 25. For all practical purposes the 5/8-in. and 3-in. DT comparison represents a comparison between geometrically similar specimens.

6-in. DT Investigations

A full-thickness DT investigation was conducted with the 6-in. A533-B Class 2 plate material. The results of the WR survey, along with the fracture surfaces, are shown in Fig. 27 (and Table A13). The same type of transition behavior is displayed for the specimens as for the 3-in. DT specimens (Fig. 25); the transition region exhibits an order-of-magnitude increase in energy absorption over a 160° F (89° C) temperature interval, and the rate of energy increase in the toe region of the curve is depressed in a similar

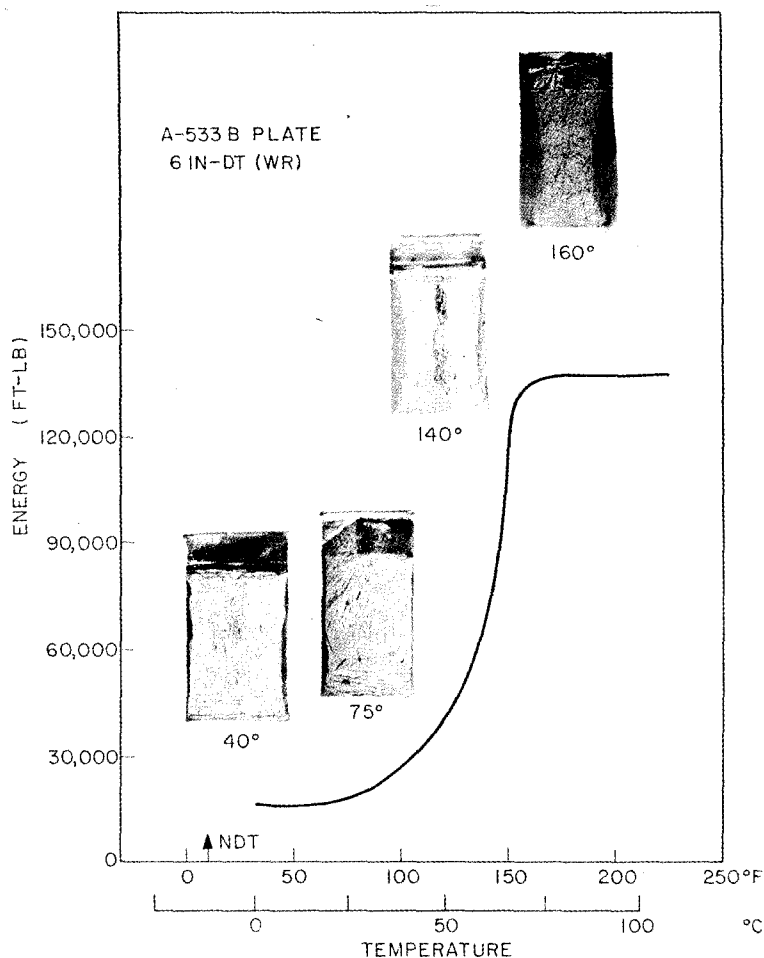


Fig. 27 - Characteristic full-plate-thickness DT energy curve for a 6-in. A533-B Class 2 plate along with the fracture surfaces of the WR specimen orientation

fashion to the 3-in. DT behavior compared with the 5/8-in. and 1-in. curves (Figs. 16 and 23). Note that the shelf-level specimen in Fig. 27 displays a large flat fibrous region approximately 3-in. wide. This trend is similar to that displayed by the 3-in. DT shelf specimens from this plate in the RW and WR orientations.

A complete 6-in. DT survey was not obtained in the RW orientation. An extrapolation of the results obtained in the transition region is shown in Fig. 28. The shelf value was obtained from the trend of E/A versus thickness displayed by other size specimens, to be discussed later (Fig. 39). The incomplete fracture noted in Fig. 28 exceeded the capacity of the large drop-weight facility (then 161,000 ft-lb). The partial fracture of this specimen, illustrated in Fig. 29, shows evidence of high ductility. Note the region of lateral contraction at the base of the notch amounting to 3/16-in. on each surface. Non-destructive examination indicated that the fracture tunneled to a depth of 5-1/2 in. below the base of the crack starter weld.

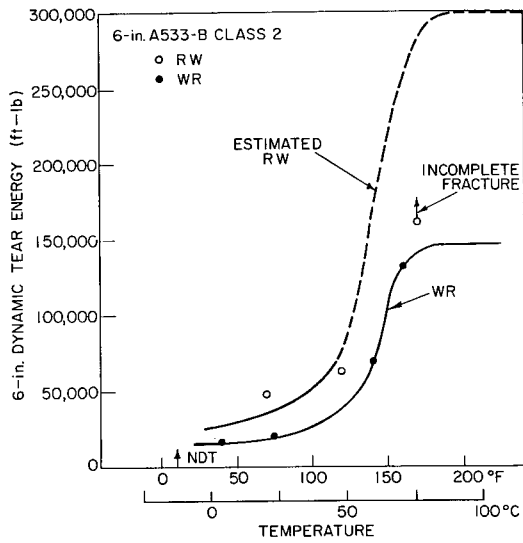


Fig. 28 - 6-in. DT comparison of the toughness variations in the RW and WR orientations for a 6-in. A533-B Class 2 plate. The shelf-level trend of the RW curve was obtained from the variation of energy/area versus specimen thickness (to be shown in Fig. 39).

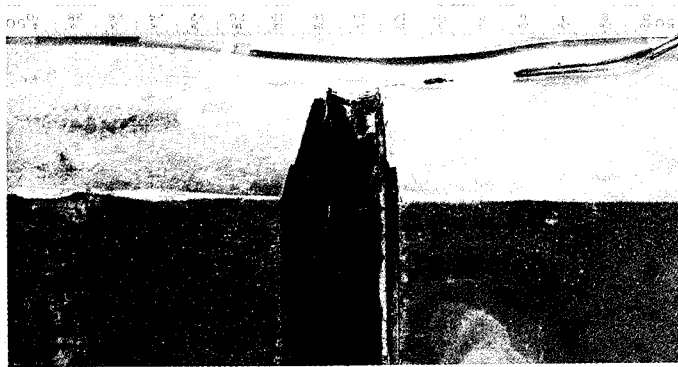
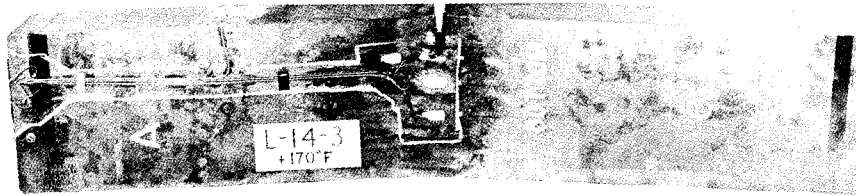


Fig. 29 - High fracture toughness of a 6-in. A533-B steel plate (full-thickness DT) tested at 170°F (77°C) in the RW orientation. The energy delivered was inadequate to develop a complete fracture (see Fig. 28). Notch blunting and lateral dimpling are evident from the lower photograph.

12-in. DT Investigations

The 12-in. DT specimen represents full-thickness material from HSST plate 01 and was the largest size investigated. Five RW specimens were fractured in the transition region. An additional 12-in. specimen was reduced to 10-in. thickness. The results of the 12-in. DT investigation are shown in Fig. 30 (and Table A14). A sharp transition involving more than an order-of-magnitude energy absorption is readily apparent in the transition region. The upswEEP begins near the NDT temperature, similar to the thinner specimen sizes. The specimen tested at 215°F (102°C) exceeded the capacity of the machine, and nondestructive examination indicated the fracture to be about two-thirds complete. The shelf-level energy was obtained by extrapolating the trend of E/A versus thickness to be shown in Fig. 39.

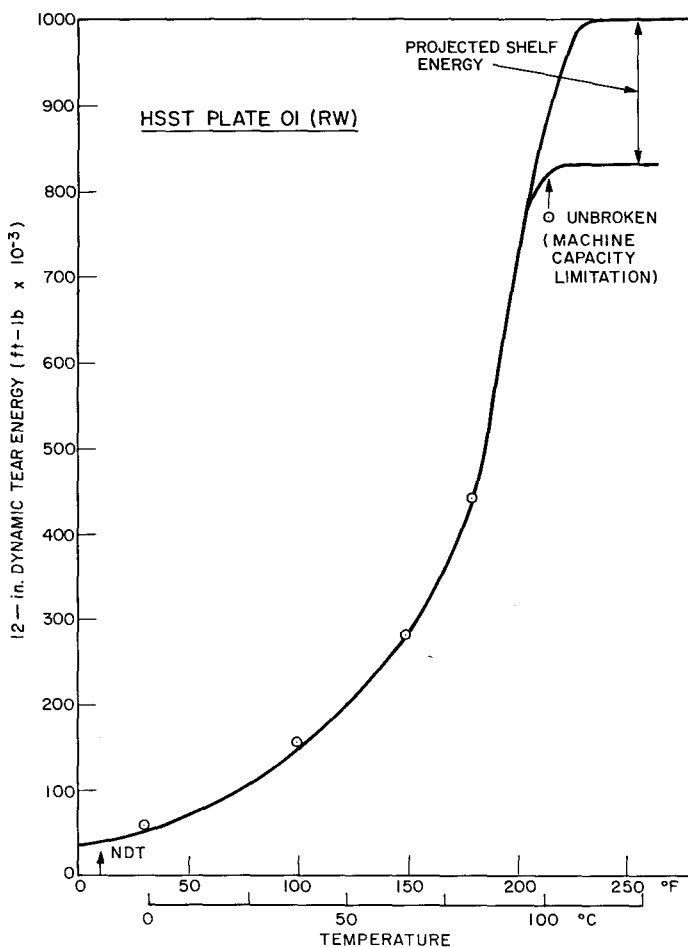


Fig. 30 - Dynamic tear energy behavior for 12-in. DT specimens cut from a 12-in. A533-B Class 2 plate (HSST plate 01) in the RW orientation. The upper shelf energy has been estimated from the trend of energy/area versus specimen thickness (to be shown in Fig. 39).

The surfaces of the completed fractures are illustrated in Fig. 31. The 30°F fracture displays a larger shear lip than normally found for fractures near the NDT. This is explained by the tough surface skin, which had a much lower NDT than the bulk of the thickness so that this material displayed essentially shelf-level toughness at the test temperature. (The dark streak on the 30°F fracture is a rust marking.)

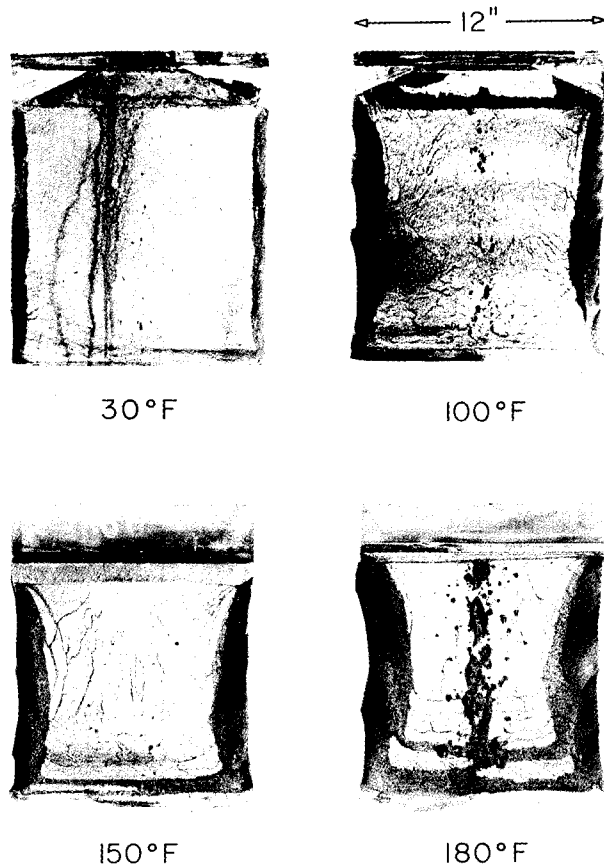


Fig. 31 - Fracture surfaces of the 12-in. DT specimens from the 12-in. A533-B Class 1 plate (HSST plate 01) plotted in Fig. 30

High-speed motion pictures were obtained for the 100°F (38°C) fracture (Fig. 31). The camera was operating at 19,000 images per second during the event. The timing marks on the film indicated the surface crack velocity to have been a maximum of 130 ft/sec. This is more than an order of magnitude slower than the crack speeds normally associated with a brittle fracture.

The shear lip size increases progressively with temperature from 1/2 in. at 30°F (-1°C) to approximately 2 in. at 180°F (82°C). The shear lip is bounded by a somewhat narrower flat fibrous region in all cases which encloses an area of cleavage. Note the presence of arrest markings at the higher temperatures. A different view of the specimen fracture at 180°F (82°C), Fig. 32, illustrates the extent of the lateral contraction, shown by the distortion from the base of the scale. The partial fracture of the specimen tested at 215°F (102°C) is shown in Fig. 33. A large lateral dimple (7/16 in. deep) is

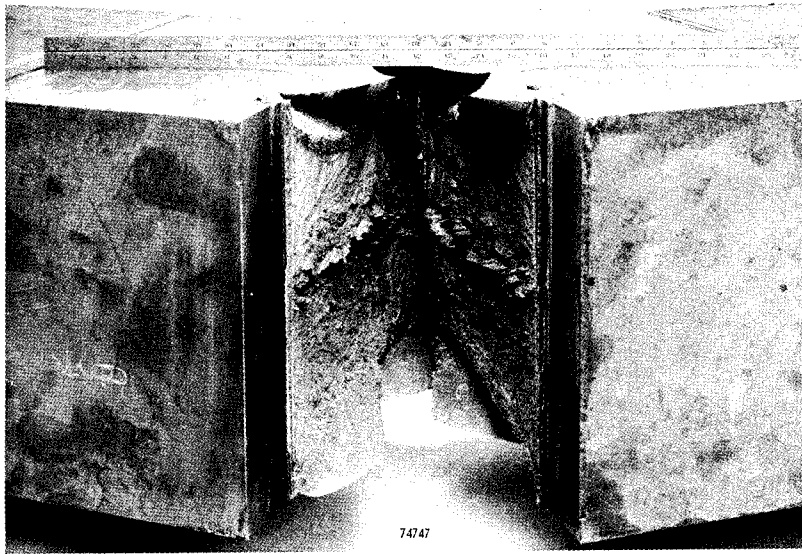


Fig. 32 - The 12-in. DT specimen fractured at 180°F (82°C), shown in Fig. 31, illustrating the lateral dimple in the fracture path. Visible deformations under the scale show a deformed area over 8 in. wide.

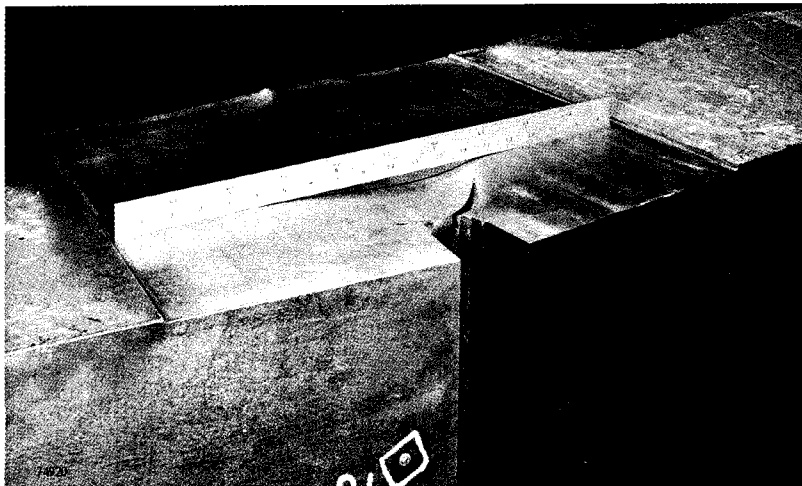
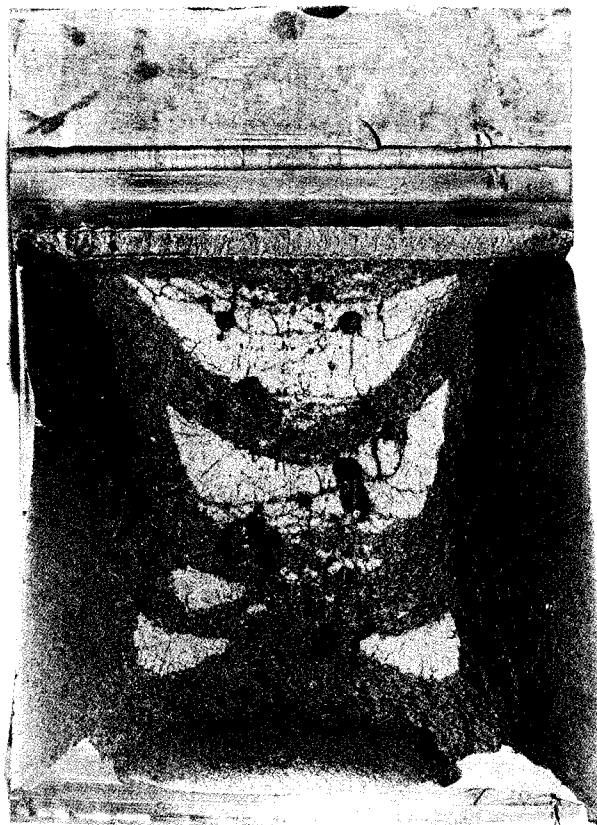


Fig. 33 - The 12-in. DT specimen which was partially fractured at 215°F (102°C) (see Fig. 30). The scale indicates the large lateral dimple in the fracture path. Visible deformations under the scale show a deformed area over 1 ft wide.

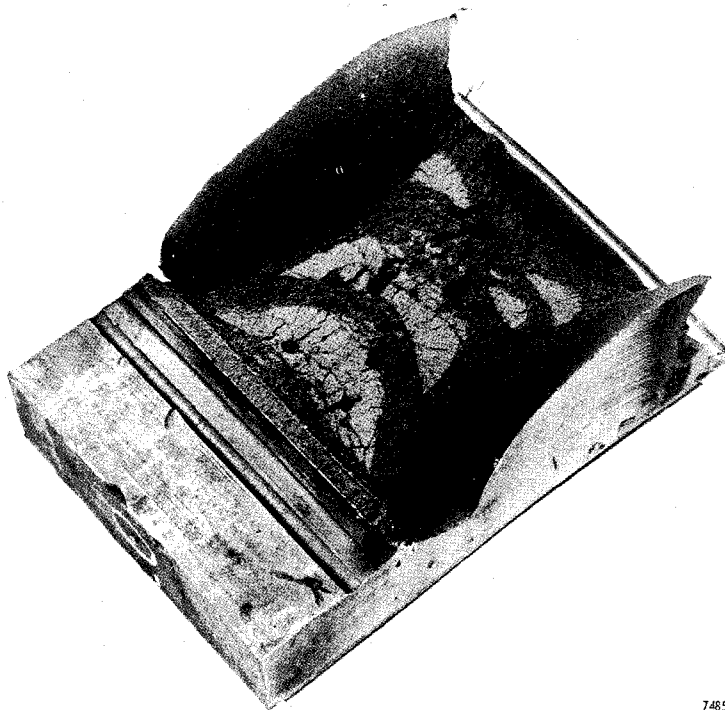
displayed at the base of each side of the crack starter notch. Further evidence of a high degree of plastic deformation is provided by measurement of the extent of the dimpled region (similar to that illustrated by the scale in Fig. 32) which extended over 6 in. on each side of the crack path.

A 10-in. DT specimen was machined from a 12-in. blank to obtain a complete fracture near the upper shelf, since the 12-in. test at 215°F (102°C) exceeded the machine capacity. The specimen energy absorption was 470,000 ft-lb; the dimensions are found in Table 1. The fracture surface is illustrated in Figs. 34 and 35. The presence of cleavage at the 220°F (104°C) test temperature indicates that the shelf temperature was not quite obtained. However, it is estimated that the shelf temperature was not more than 10 to 15°F (6 to 8°C) above the test temperature. The specimen tested at 215°F (102°C) shows evidence of lamination near the midthickness plate similar to the 180°F (82°C) fracture in Fig. 31. This resulted in a certain loss of constraint which probably permitted shelf conditions to be obtained at a somewhat lower temperature than that for the 10-in. DT which did not exhibit laminations to this degree.



74853

Fig. 34 - Fracture surface of a 10-in. DT specimen cut from a 12-in. A533-B Class 1 steel plate by removing 1-in. of material from each plate surface. The RW specimen was tested at 220°F (104°C). The surface contains approximately 15% cleavage.



74852 205

Fig. 35 - Oblique view of the 10-in. DT fracture surface shown in Fig. 34 illustrating shear lips approximately 2 in. thick on each surface

SIZE EFFECT INTERPRETATIONS

The results of DT investigations indicate that a sharp transition from brittle to ductile behavior is displayed for all specimen sizes. This transition is reflected by a change in the fracture mode from cleavage to dimpled rupture. Indications of a thickness effect, however, become evident by the depression in the rate of increase in energy in the lower toe region of the DT curves for the thicker sizes (≥ 3 in.) compared with the trend of the 5/8- and 1-in. DT specimens. Further evidence for this size effect is given by a composite photo of fracture surfaces of the 5/8-, 3-, and 6-in. specimens (Figs. 16, 25, and 27) illustrated in Fig. 36. The lines separate the fractures by energy into the three regimes previously defined. The changes in fracture appearance clearly reflect the increase in energy absorption and show a transition from flat fractures with small shear lips (regime 1), to fractures containing slight and then strong arrest markings (regime 2), and finally to fractures indicating a large lateral contraction and rapidly increasing areas of fibrous tearing. The change in fracture appearance through regime 2 occurs dramatically in a narrow temperature range. The development of arrest markings is shifted to higher temperatures for thicker specimens, thereby indicating a size effect.

The development of a high degree of lateral contraction on the upper shelf for all specimen sizes, coupled with a transition to fibrous fracture associated with an order-of-magnitude increase in energy absorption in the transition region, leads to the conclusion that unstable fracture is no longer possible at shelf-level temperature. Hence regime 3 is taken to indicate fracture under plastic overload for the thick specimens similar to the interpretation for thinner specimens previously set forth. The definition

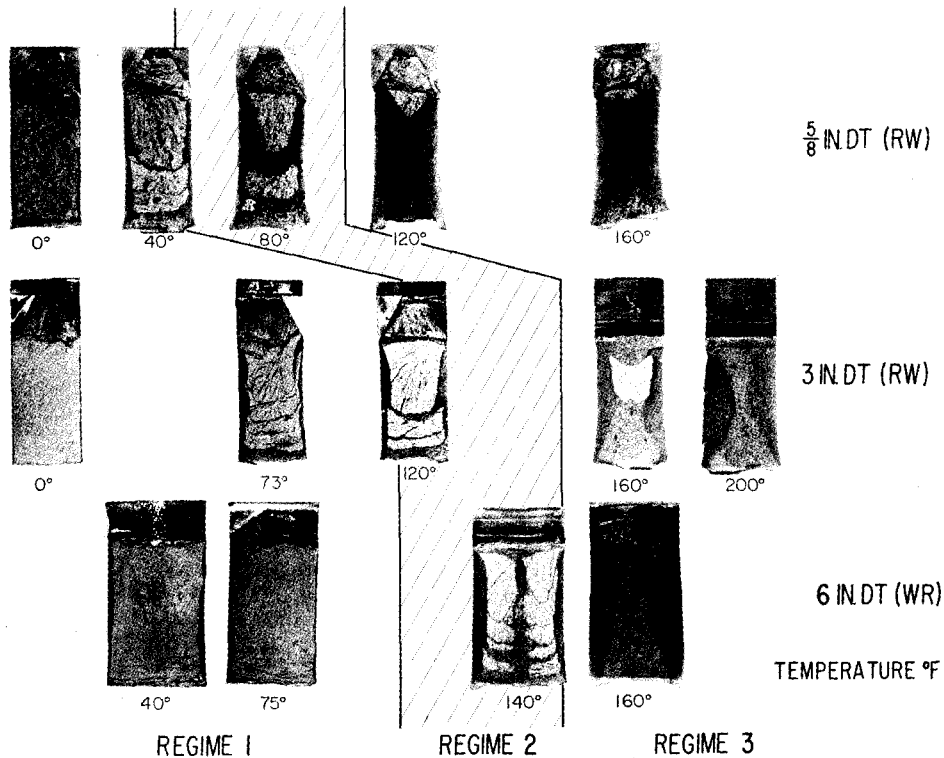


Fig. 36 - Composite photo of the fracture surfaces of 5/8-, 3-, and 6-in. DT specimens shown in Figs. 16, 25, and 27. The fractures are divided into the three toughness regimes to be illustrated in Figs. 37 and 38. Featureless, flat fractures of regime 1 are extended to higher temperatures by increased thickness. The arrest markings indicate a transition through regime 2. Fibrous fractures and lateral contraction fractures indicate completion of regime 3 of the transition.

of the fracture transition — elastic (FTE) at the 50% energy level is therefore retained for thicker specimens.

The magnitude of the size effect is defined as the temperature shift in the FTE as a function of specimen thickness. This shift can be determined from the various graphs presented. For ease in interpretation these graphs are replotted on a normalized E/A basis for the 6-in. A533-B Class 2 plate (Fig. 37) and for the 12-in. A533-B Class 1 plate (Fig. 38). To obtain these plots the shelf E/A (using the unbroken ligament area) was taken as unity and the remainder of the curve was plotted accordingly. This method of representation makes it easier to define the temperature associated with each of the toughness regimes. It is felt that regime 1 is indicative of the same type of brittle fracture performance for all sizes of specimens. In regime 3, however, there appear to be differences in the extent of plastic deformation between the different sizes. These differences in energy absorption cannot at present be related to the plastic load carrying capacity of a structure. The fact that plastic deformation is evident for all specimens at shelf temperatures permits the adoption of a common regime 3 nomenclature.

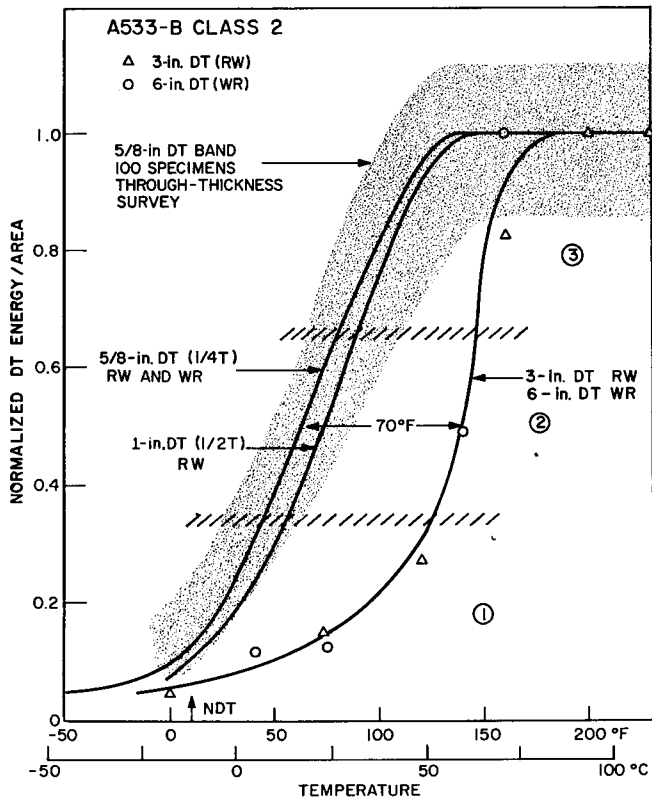


Fig. 37 - DT test curves for specimens of various thicknesses from a 6-in. A533-B Class 2 steel. The specimen trends are normalized on the basis of upper shelf energy/fractured area. The normalization procedure indicates a size effect by the shift in the FTE (DT energy midpoint) with thickness.

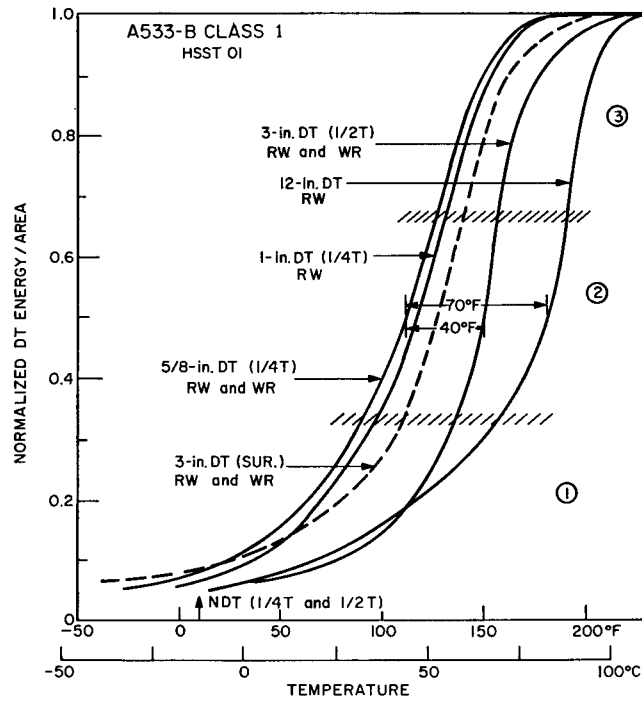


Fig. 38 - DT test curves for specimens of various thicknesses from a 12-in. A533-B Class 1 steel plate (HSST 01). The specimen trends are normalized on the basis of upper shelf energy/fractured area. The normalization procedure indicates a size effect by the shift of the FTE (DT energy midpoint) with thickness. The behavior of the tough surface layer is indicated by the dashed 3-in. DT curve.

Figure 37 indicates a size effect of approximately 70° F (39° C) between the 5/8-in. and 1-in. specimens and the 3-in. and 6-in. specimens. Very little difference between the FTE of the 5/8- and 1-in. specimens is noted; the same is true for the 3- and 6-in. specimens. The mechanical constraint associated with the thicker specimens suppresses the initial increase in toughness of regime 1, however, the rates of increase in regime 2 and 3 are not affected.

A similar comparison for the 12-in. A533-B Class 1 plate (Fig. 38) indicates a 40° F (22° C) size effect between the 5/8-in. and 3-in. DT specimens from the 1/2 T location for both RW and WR orientations. The 3-in. DT curve from surface material is plotted for comparison. The size effect for this location can be approximated from the 5/8-in. and 1-in. DT curves for surface material (Figs. 7 and 22). The comparison is not clear-cut because of the metallurgical gradient in toughness which is integrated by the 3-in. specimen but not by the thinner specimens. The 12-in. DT specimen exhibits a size effect of approximately 70° F (39° C). Note that the 3-in. (1/2 T) curve intersects the 12-in. DT curve in regime 1. This occurs because the 12-in. DT specimen is affected by the tough surface skin (indicated by the dashed 3-in. curve). However, the 12-in. curve is displaced to higher temperature, as the differences between the toughness of surface and midthickness material decrease with increasing temperature.

A comparison of the trends in energy density (E/A) as a function of thickness is illustrated in Fig. 39. Since the data are presented as a function of the log of specimen thickness, a distinct tendency toward "saturation" of energy density is evident. This tendency is reflected in the fracture appearance. Smaller size specimens of high toughness result in full slant fractures at the shelf temperatures; thicker specimens show a tendency for shear lips to occupy only a portion of the fracture mode (Fig. 36). The trend toward saturation is further emphasized by the bottom curve. This method of representation illustrates that the upper-shelf energy absorption is strongly dependent on the metallurgical quality of the steel as exhibited by the variation between the curves for RW and WR orientations. Even for a given orientation the differences between surface and midthickness material are clearly evident (e.g., the spread in the 3-in. DT data).

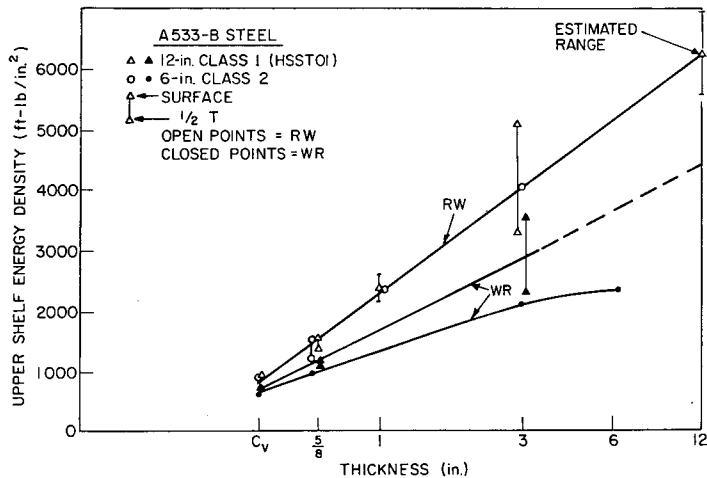


Fig. 39 - Trend of DT upper shelf energy/area with specimen thickness. The importance of metallurgical quality on shelf-level toughness is apparent from the trends of RW and WR orientations. A trend toward saturation of energy/area with specimen thickness is evident.

COMPARISON OF DT TESTS WITH FRACTURE MECHANICS

Westinghouse Research Laboratories investigators have completed the large-size K_{Ic} tests required to resolve the constraint effects issue as related to fracture mechanics parameters. The results of compact tension specimens (CTS) of thicknesses up to 12 in. for a plate of A533-B steel (HSS1 plate 02) are presented in Fig. 40 (9) and are compared with the 12-in. DT results from HSS1 plate 01. The K_{Ic} data clearly indicate a sharp increase with temperature which begins near NDT. Valid K_{Ic} numbers (according to ASTM Committee E-24 recommendations) were not obtained at temperatures above 50° F (10° C), at which point a K_{Ic}/σ_{ys} ratio of 2.0 was measured, requiring a 12-in.-thick specimen. The infinity (∞) notation on the K_{Ic} curve signifies a projection to infinitely high ratios and corresponding large increases in critical flaw sizes within a small temperature increment. In effect, this denotes the highest temperature for which static linear elastic fracture mechanics is applicable for this steel. For specimens less than 12 in. thick the loss of mechanical constraint will result in the limit of linear elastic behavior occurring at a correspondingly lower temperature.

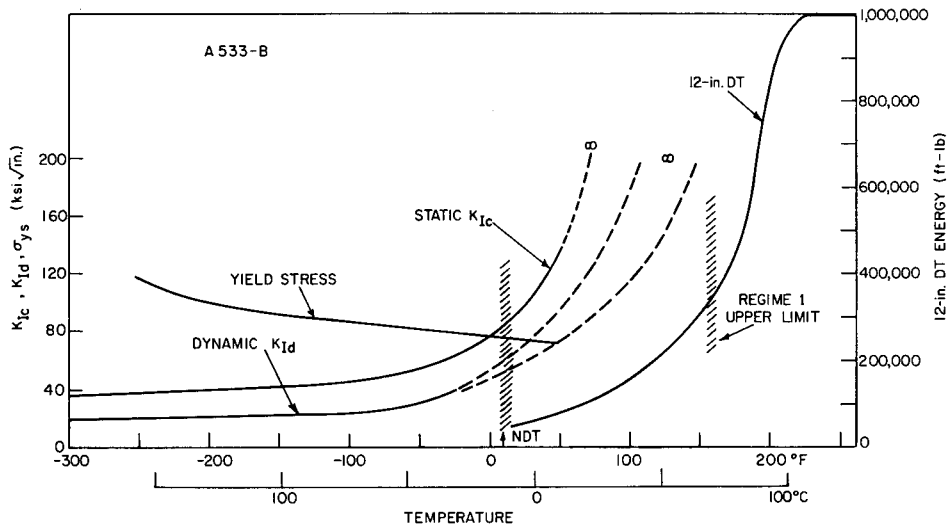


Fig. 40 - Comparison of thick-section DT tests with static (K_{Ic}) and dynamic (K_{Id}) data for A533-B steel. Large-section (12 in. thick) K_{Ic} specimens did not extend the measurement capacity of static plane strain fracture toughness beyond $NDT + 40^\circ F$ ($22^\circ C$). K_{Id} values are extrapolated to higher temperatures, but it is evident from the sharply rising region of the thick-section DT curve, that K_{Id} specimens of large size would not extend the measurement capability beyond the limit defined by the DT tests.

The transitional behavior of the K_{Ic} data corroborates the trend displayed by the thick-section DT tests. It is apparent that some temperature below the FTE must define the limit of dynamic linear elastic conditions for the thickness in question. This limit is chosen as the upper temperature boundary of the DT regime 1, since regime 2 (containing the FTE) defines a regime where yield stress loads are required to propagate a fracture. The temperature of $150^\circ F$ ($66^\circ C$) therefore represents a conservative upper boundary for dynamic K_{Id} tests for HSSST plates 01 and 02. Unfortunately, thick-section dynamic K_{Id} data do not exist which can be used to verify this conclusion. Figure 40 illustrates an extrapolation of existing dynamic K_{Id} data on A302-B steel* to show the expected behavior at high temperatures (3).

The projected K_{Id} upper limit for dynamic loading must occur at a higher temperature than the $50^\circ F$ ($10^\circ C$) K_{Ic} limit for static loading because of the strain rate sensitivity of the A533-B steel. A tentative verification of the fact that $150^\circ F$ ($66^\circ C$) corresponds to the upper temperature limit for dynamic LEM tests is obtained from two sources. Barsom and Rolfe (10) define a method for predicting K_{Id} behavior by a lateral shift in temperature of the K_{Ic} curve based on thin-section tests. The magnitude of this shift is obtained from static and dynamic Charpy-V data (both regular and fatigue cracked C_v specimens). If applicable to thick sections, this method would shift the static K_{Ic} curve for A533-B by $100^\circ F$ ($55^\circ C$) and thereby project the temperature limit for valid K_{Id} data as $150^\circ F$ ($66^\circ C$). Another method by Witt (11) would shift the static K_{Ic} curve by $80^\circ F$ ($33^\circ C$) to put the K_{Id} limit at $130^\circ F$ ($54^\circ C$). This shift is defined from the projection (to 12-in. specimens) of the break/no-break condition of drop-weight type specimens (i.e., geometrically scaled from the ASTM E-208 standard specimen) conducted under another

*The A302-B data are believed to be representative of that for A533-B. These data are adjusted to the NDT of the A533-B plates indicated in Fig. 40.

phase of the HSST Program (12). For the design of the drop-weight specimen the highest temperature of a "no break" under impact corresponds to plastic deformation throughout the specimen thickness.

SUMMARY

The effect of mechanical constraint imposed by thick sections has been examined in the framework of linear elastic fracture mechanics and other transition temperature indices. Extrapolations of thin-section linear elastic fracture mechanics (LEFM) data to higher temperatures has raised the concern that thick-section steels, of shelf toughness and strength class similar to A533-B, will not exhibit a transition temperature behavior. The research programs at NRL relating to thick DT studies and those at Westinghouse relating to thick LEFM investigations have shown that unirradiated A533-B does exhibit a significant increase in toughness within a relatively narrow temperature region near the NDT.

For the steels investigated the DT energy curve may be divided into three toughness regimes which are shown to indicate similar fracture transition features for specimens 5/8 in. to 12 in. thick. Regime 1 defines a temperature interval of rapidly increasing dynamic LEFM fracture toughness which eventually renders this technique inapplicable with small increases in temperature. Regime 3 represents fracture exhibiting large plastic deformation for which suitable fracture mechanics analyses have not yet been developed. Regime 2 defines a transition between the two extreme cases in which nominal stresses above yield level become necessary to propagate fracture. The midpoint energy, located in this regime, is defined as the fracture transition — elastic (FTE) for steels of the A533 toughness level.

The DT size-effect studies indicate that thick sections continue to exhibit a brittle-ductile transition, similar to that of thin sections, involving more than an order-of-magnitude increase in energy absorption. Material used at temperatures corresponding to regime 3 cannot fail in an unstable manner under elastic loading even in the presence of very large surface flaws. Failure can only occur by a substantial degree of gross plastic deformation or under the action of elastic stresses when the flaw sizes become so large as to lead to a buckling situation (geometric instability). The size effects studies, however, do indicate that the effects of mechanical constraint associated with thick sections elevate the FTE temperature for 12-in. thick sections about 70°F (39°C) above that for thin sections. This result may require a more conservative application of existing reactor vessel operating procedures, which generally have required vessel operation under reduced pressure at temperatures below FTE defined as NDT + 60°F (33°C) for thin sections.

The temperature corresponding to the upper boundary of regime 1 represents the temperature limit of applicability for dynamic LEFM analysis for a given thickness. It is concluded from the rapid increase in DT fracture toughness at this temperature that a correspondence with rapidly increasing ratios of dynamic K_{Ic}/σ_{ys} and associated critical flaw sizes of large proportions must exist. It also is concluded that the behavior exhibited by the DT test is the result of fundamental processes related to increases in microfracture ductility which determine the existence of a temperature-induced transition regardless of test procedure. Accordingly, large-size dynamic K_{Ic} tests must also project a fracture toughness transition which leads to the requirements of plastic loading for fracture similar to that of the static K_{Ic} results described.

REFERENCES

1. Text of ACRS Letter to AEC, Nucleonics 24(No. 1), 17 (Jan. 1966)
2. Pellini, W.S., and Puzak, P.P., "Fracture Analysis Diagram Procedures for the Fracture-Safe Engineering Design of Steel Structures," NRL Report 5920, Mar. 15, 1963; Welding Res. Council Bull. Ser. 88 (1963)
3. Loss, F.J., and Pellini, W.S., "Coupling of Fracture Mechanics and Transition Temperature Approaches to Fracture-Safe Design," NRL Report 6913, Apr. 14, 1969; Proceedings of Symposium on Fracture Toughness Concepts for Weldable Structural Steels, Culcheth, England, Apr. 29-30, 1969; "Practical Fracture Mechanics for Structural Steel," Chapman and Hall, Aug. 1969
4. Pellini, W.S., and Loss, F.J., "Integration of Metallurgical and Fracture Mechanics Concepts of Transition Temperature Factors Relating to Fracture-Safe Design for Structural Steels," NRL Report 6900, Apr. 22, 1969; Welding Res. Council Bull. 141, June 1969
5. "HSST Program - Semi-Annual Progress Report for Period Ending February 29, 1968," ORNL-4315, Oak Ridge National Laboratory, Oct. 1968
6. "HSST Program - Semi-Annual Progress Report for Period Ending 31 August 1968," ORNL-4377, Oak Ridge National Laboratory, Apr. 1969
7. "HSST Program - Semi-Annual Progress Report for Period Ending 28 February 1969," ORNL-4463, Oak Ridge National Laboratory, Jan. 1970
8. "HSST Program - Semi-Annual Progress Report for Period Ending 31 August 1969," ORNL-4512, Oak Ridge National Laboratory, Mar. 1970.
9. Wessel, E.T., "Linear Elastic Fracture Mechanics for Welded Steel Pressure Vessels: Material Property Considerations," Proceedings of Symposium on Fracture Toughness Concepts for Weldable Structural Steels, Culcheth, England, Apr. 29-30, 1969; "Practical Fracture Mechanics for Structural Steel," Chapman and Hall, Aug. 1969
10. Barsom, J.M., and Rolfe, S.T., "Correlations Between K_{Ic} and Charpy-V Notch Test Results in the Transition Temperature Range," presented at ASTM Symposium on Impact Testing of Metals, June 22-27, 1969, Atlantic City, N.J.; ASTM Special Technical Publication 466 Mar. 1970
11. Witt, F.J., "Preliminary Interpretations of the Size Effects in Dynamic Tear Specimens Based on Both Strength and Transition Temperature Approaches," Heavy Section Steel Technology Program Special Report, July 14, 1969, Oak Ridge National Laboratory (unpublished)
12. Loechel, L.W., "The Effect of Section Size on the Transition Temperature in Steel," Heavy Section Steel Technology Program, HSSTP-TR-2, Nov. 20, 1969, Oak Ridge National Laboratory

Appendix A

TABULATIONS OF THE DATA

- Table A1 – Data Plotted in Figs. 7 and 8: DT Energy Values (RW Orientation) From a 12-in. A533-B Steel Plate (HSST 01)
- Table A2 – Data Plotted in Figs. 10 and 11: 5/8-in. DT Energy Values From a 12-in. A533-B Steel Plate (HSST 02)
- Table A3 – Data Plotted in Figs. 12 and 14: 5/8-in. DT Energy Values (RW Orientation, Machined-Notch Crack Starters) From a 12-in. A533-B Steel Plate (HSST 03)
- Table A4 – Data Plotted in Fig. 15: 5/8-in. DT Energy Values From a 12-in. A533-B Class 1 Plate (HSST 01) in the RW Orientation at Elevated Temperature (Specimens From Location D in Fig. 7 From the Bottom Half of the Plate Thickness and With EB-Weld Crack Starters)
- Table A5 – Data Plotted in Figs. 16 and 18: 5/8-in. DT Energy Values For a 6-in. A533-B Class 2 Steel Plate
- Table A6 – Data Plotted in Fig. 19: 5/8-in. DT Energy Values (EB-Weld Crack Starters) From a 12-in. Submerged Arc Weld Formed With A533 Steel (HSST Plate 01; HSST Weld 50)
- Table A7 – Data Plotted in Fig. 21: 5/8-in. DT Energy Values (EB-Weld Crack Starters) From a 6-in. Electroslag Weld Formed With A533 Steel (HSST Weld 53)
- Table A8 – Data Plotted in Fig. 22: 1-in. DT Energy Values From a 12-in. A533-B Class 1 Steel Plate (HSST 01) in the RW Orientation (EB-Weld Crack Starters)
- Table A9 – Data Plotted in Fig. 23: 1-in. DT Energy Values From a 6-in. A533-B Class 2 Steel Plate in the RW Orientation
- Table A10 – Data Plotted in Fig. 24: 3-in. DT Energy Values From a 12-in. A533-B Class 1 Steel Plate (HSST 01)
- Table A11 – Data Plotted in Fig. 25: 3-in. DT Energy Values From a 6-in. A533-B Class 2 Steel Plate (Each Specimen Spanning From the Surface to Mid-thickness)
- Table A12 – DT Energy Values From a 6-in. A533-B Class 2 Steel Plate Using Special 3-in. Specimens Geometrically Similar to the 5/8-in. DT Specimen and Spanning From the Surface to Midthickness (RW Orientation)
- Table A13 – Data Plotted in Fig. 27: 6-in. DT Energy Values From a 6-in. A533-B Class 2 Steel Plate
- Table A14 – Data Plotted in Fig. 30: 12-in. DT Energy Values From a 12-in. A533-B Class 1 Steel Plate (HSST 01) With the Specimens Oriented in the RW Direction

Table A1
Data Plotted in Figs. 7 and 8: 5/8-in. DT Energy Values (RW Orientation)
From a 12-in. A533-B Steel Plate (HSST 01)

Location* (see Fig. 7)	Temperature		Specimen Number		DT Energy (ft-lb)		Location* (see Fig. 7)	Temperature		Specimen Number		DT Energy (ft-lb)	
	°F	°C	Electron Beam Weld	Machined Notch	Electron Beam Weld	Machined Notch		°F	°C	Electron Beam Weld	Machined Notch	Electron Beam Weld	Machined Notch
A	-120	-84	L-83-A2	L-83-A13	54*	65*	E	50	10		E1-5		213*
	-100	-73		E1-1		100*		80	27	L-83-E2	L-83-E13	271*	259*
	-80	-62	L-83-A4	L-83-A17	92	92		100	38	L-83-E4	L-83-E17	385	480
	-60	-51	L-83-A5	L-83-A14	224*	167*		120	49	L-83-E5	L-83-E14	537*	568*
	-40	-40	L-83-A9	L-83-A18	334	732		120	49		E1-22		571*
	-20	-29	L-83-A6	L-83-A15	603*	652*		140	60	L-83-E9	L-83-E18	812	891
	0	-18	L-83-A10	L-83-A19	905	973		160	71	L-83-E6	L-83-E15	1039*	1061*
	0	-18		E1-34		994		160	71		E1-13		1044
	40	4	L-83-A7	L-83-A16	998*	1033*		180	82	L-83-E10	L-83-E19	1184	970
	80	27	L-83-A11	L-83-A20	1016	1044		200	93	L-83-E7	L-83-E16	1073*	1143*
	80	27		E1-18		1002*		200	93		E1-30		1070
	120	49	L-83-A8		1065*			220	104	L-83-E11	L-83-E20	1076	1052
	160	71		E1-17		990		240	116	L-83-E8	L-83-E12	1215*	995
	B	-80	-62	L-83-B2	L-83-B13	54*		59*	F	-40	-40	L-83-F2	L-83-F13
-40		-40	L-83-B4	L-83-B17	87	97	0	-18		L-83-F4	L-83-F17	80	80
0		-18	L-83-B5	L-83-B14	219*	163*	40	4		L-83-F5	L-83-F14	157*	130*
0		-18		E1-2		172*	80	27		L-83-F9	L-83-F18	335	245
40		4	L-83-B9	L-83-B18	499	325	80	27			E1-6		284*
50		10		E1-33		456	80	27			E1-23		266*
60		16	L-83-B6	L-83-B15	559*	360*	80	27			E1-12		293
80		27	L-83-B10	L-83-B19	760	668	80	27			E1-29		256
80		27		E1-19		810*	120	49		L-83-F6	L-83-F15	517*	608*
120		49	L-83-B7	L-83-B16	973*	974*	140	60		L-83-F10	L-83-F19	745	933
160		71	L-83-B11	L-83-B20	1110	1110	160	71		L-83-F7	L-83-F16	943*	985*
160		71		E1-16		1064	180	82		L-83-F11	L-83-F20	1067	986
200		93	L-83-B8	L-83-B12	1038*	1131	210	99		L-83-F8	L-83-F12	1008*	1025
C		-40	-40	L-83-C2	L-83-C13	53*	63*	G		0	-18		E1-6
	0	-18	L-83-C4	L-83-C17	105	102	80		27	L-83-G2	L-83-G13	310*	261*
	0	-18		E1-20		113*	80		27		E1-24		258*
	40	4	L-83-C5	L-83-C14	207*	177*	100		38	L-83-G4	L-83-G17	447	395
	80	27	L-83-C9	L-83-C18	393	447	120		49	L-83-G5	L-83-G14	522*	451*
	80	27		E1-15		423	140		60	L-83-G9	L-83-G18	761	707
	120	49	L-83-C6	L-83-C15	913*	832*	160		71	L-83-G6	L-83-G15	890*	858*
	140	60	L-83-C10	L-83-C19	1183	951	160		71		E1-11		1027
	160	71	L-83-C7	L-83-C16	1054*	1090*	180		82	L-83-G10	L-83-G19	1055	1068
	160	71		E1-3		991*	200		93	L-83-G7	L-83-G16	1024*	1059*
	180	82	L-83-C11	L-83-C20	1147	1139	200		93		E1-28		1093
	200	93		E1-32		1093	220		104	L-83-G11	L-83-G20	1142	1166
	210	99	L-83-C8	L-83-C12	1138*	1081	240		116	L-83-G8	L-83-G12	1081*	1090
	D	-40	-40	L-83-D2	L-83-D13	56*	59*		H	-40	-40	L-83-H2	L-83-H13
0		-18	L-83-D4	L-83-D17	95	84	0	-18		L-83-H4	L-83-H17	72	58
40		4	L-83-D5	L-83-D14	178*	168*	0	-18			E1-25		83*
50		10		E1-31		215	40	4		L-83-H5	L-83-H14	135*	138*
80		27	L-83-D9	L-83-D18	416	272	80	27		L-83-H9	L-83-H18	306	301
80		27		E1-4		296*	80	27			E1-10		286*
120		49	L-83-D6	L-83-D15	751*	838*	120	49		L-83-H6	L-83-H15	530*	497*
120		49		E1-21		675*	140	60		L-83-H10	L-83-H19	700	748
140		60	L-83-D10	L-83-D19	913	978	160	71		L-83-H7	L-83-H16	899*	877*
160		71	L-83-D7	L-83-D16	1070*	1091*	160	71			E1-27		847
160		71		E1-14		1224	180	82		L-83-H11	L-83-H20	927	938
180		82		L-83-D20		1080	200	93			E1-8		972*
180		82		L-83-D11		1256	210	99		L-83-H8	L-83-H12	987*	985
210		99	L-83-D8	L-83-D12	1051*	1125							
I	40	4	L-83-I2	L-83-I6	143	162		80	27	L-83-I3	L-83-I7	434	299
	120	49	L-83-I4	L-83-I8	616	707		120	49		E1-26		558
	120	49		E1-26		558		160	71	L-83-I5	L-83-I9	815	835
	160	71		E1-9		872		160	71		E1-9		872
	160	71		E1-9		872		180	82		L-83-I10		839
	180	82		L-83-I10		839							

*The DT energy values marked with an asterisk are those of specimens cut from the top surface to the midthickness (from the right of the sketch in Fig. 7); all other values are for specimens cut from the bottom half (from the centerline and left in Fig. 7).

Table A2
Data Plotted in Figs. 10 and 11: 5/8-in. DT Energy Values
From a 12-in. A533-B Steel Plate (HSST 02)

Location (see Fig. 10)	Temperature		Specimen Number*	DT Energy (ft-lb)	Location (see Fig. 10)	Temperature		Specimen Number*	DT Energy (ft-lb)	Location (see Fig. 10)	Temperature		Specimen Number*	DT Energy (ft-lb)	
	°F	°C				°F	°C				°F	°C			
RW Orientation, Machined Notch				RW Orientation, Machined Notch				RW Orientation, Machined Notch							
A	-120	-84	L-73-A1	89	E	-40	-40	L-73-E1	57	I	120	49	L-73-I1	621	
	-80	-62	L-73-A8	133		0	-18	L-73-E8	81		140	60	L-73-I7	852	
	-60	-51	L-73-A11	235		40	4	L-73-E2	139		160	71	L-73-I5	938	
	-40	-40	L-73-A13	443		80	27	L-73-E9	275		180	82	L-73-I4	975	
	-40	-40	L-73-A2	733		100	38	L-73-E13	411		200	93	L-73-I3	1040	
	-20	-29	L-73-A5	765		120	49	L-73-E3	586		220	104	L-73-I2	1014	
	-20	-29	L-73-A14	839		120	49	L-73-E10	506		240	116	L-73-I1	984	
	0	-18	L-73-A6	994		140	60	L-73-E4	989		WR Orientation, EB Weld				
	0	-18	L-73-A9	901		160	71	L-73-E7	1119						
	20	-7	L-73-A12	979		160	71	L-73-E11	1006		A	-100	-73	L-73-A28	57
	20	-7	L-73-A7	1056		180	82	L-73-E5	1058			-80	-62	L-73-A27	83
	40	4	L-73-A3	982		200	93	L-73-E12	1020			-60	-51	L-73-A21	211
	80	27	L-73-A10	966		200	93	L-73-E14	1097			-40	-40	L-73-A26	232
	120	49	L-73-A4	1027		220	104	L-73-E6	1060			-20	-29	L-73-A20	546
B	-80	-62	L-73-B1	52	F	-40	-40	L-73-F1	49	F		40	4	L-73-F22	139
	-40	-40	L-73-B8	85		0	-18	L-73-F8	55			80	27	L-73-F23	249
	0	-18	L-73-B2	153		40	4	L-73-F2	108			100	38	L-73-F24	330
	40	4	L-73-B9	295		80	27	L-73-F9	322			120	49	L-73-F25	407
	60	16	L-73-B13	569		100	38	L-73-F3	317			140	60	L-73-F18	592
	60	16	L-73-B6	550		120	49	L-73-F10	565			160	71	L-73-F17	713
	80	27	L-73-B3	696		140	60	L-73-F4	933			180	82	L-73-F16	819
	100	38	L-73-B7	1043		140	60	L-73-F14	875			220	104	L-73-F15	808
	100	38	L-73-B12	922		160	71	L-73-F11	889			G	40	4	L-73-G22
	120	49	L-73-B10	1105		180	82	L-73-F5	1055		80		27	L-73-G23	209
	140	60	L-73-B14	1067		180	82	L-73-F7	1160		100		38	L-73-G24	361
	140	60	L-73-B5	1075		200	93	L-73-F12	958		120		49	L-73-G25	437
	160	71	L-73-B4	1144		220	104	L-73-F6	1040		140		60	L-73-G18	560
	180	82	L-73-B11	1110		240	116	L-73-F13	990		160		71	L-73-G17	729
C	-40	-40	L-73-C1	57	G	-40	-40	L-73-G1	56	H	0		-18	L-73-H15	85
	0	-18	L-73-C8	92		0	-18	L-73-G8	60		40		4	L-73-H16	157
	40	4	L-73-C2	219		40	4	L-73-G2	110		40		4	L-73-H22	157
	80	27	L-73-C9	361		80	27	L-73-G9	332		80		27	L-73-H17	290
	80	27	L-73-C7	379		100	38	L-73-G3	330		120		49	L-73-H18	446
	100	38	L-73-C3	806		120	49	L-73-G10	549		160		71	L-73-H23	759
	120	49	L-73-C10	986		140	60	L-73-G4	652		180		82	L-73-H24	777
	120	49	L-73-C13	1043		160	71	L-73-G11	1058		220		104	L-73-H25	799
	140	60	L-73-C4	1036		160	71	L-73-G7	960		I	80	27	L-73-I14	301
	160	71	L-73-C11	1114		180	82	L-73-G5	1030			120	49	L-73-I13	439
	160	71	L-73-C14	1059		180	82	L-73-G12	991			140	60	L-73-I12	584
	180	82	L-73-C5	1077		200	93	L-73-G12	991			160	71	L-73-I11	700
	200	93	L-73-C12	1038		200	93	L-73-G14	1004			180	82	L-73-I10	749
	220	104	L-73-C6	1087		220	104	L-73-G6	1004			200	93	L-73-I9	710
D	-40	-40	L-73-D1	51	H	0	-18	L-73-H1	77	220		104	L-73-I8	789	
	0	-18	L-73-D8	75		40	4	L-73-H8	133	I		80	27	L-73-I14	301
	40	4	L-73-D1	143		80	27	L-73-H2	332			120	49	L-73-I13	439
	60	16	L-73-D9	199		100	38	L-73-H9	396			140	60	L-73-I12	584
	80	27	L-73-D3	313		120	49	L-73-H3	663			160	71	L-73-I11	700
	80	27	L-73-D10	348		120	49	L-73-H7	559			180	82	L-73-I10	749
	100	38	L-73-D4	441		140	60	L-73-H10	716			200	93	L-73-I9	710
	120	49	L-73-D11	738		160	71	L-73-H14	997			220	104	L-73-I8	789
	140	60	L-73-D5	1048		160	71	L-73-H4	955		I	80	27	L-73-I14	301
	140	60	L-73-D12	1118		180	82	L-73-H11	1042			120	49	L-73-I13	439
	160	71	L-73-D6	1017		180	82	L-73-H5	984			140	60	L-73-I12	584
	180	82	L-73-D13	973		200	93	L-73-H5	984			160	71	L-73-I11	700
	200	93	L-73-D7	1076		200	93	L-73-H13	1001			180	82	L-73-I10	749
	220	104	L-73-D14	1024		220	104	L-73-H12	1061			200	93	L-73-I9	710
				240	116	L-73-H6	997	220	104			L-73-I8	789		

*In the specimen number L-73-XYX, X indicates the location, YY = 1-7 and 15-21 indicates that the location is in the top half of the plate, and YY = 8-14 and 22-28 indicates that the location is in the bottom half of the plate.

Table A3
Data Plotted in Figs. 12 and 14: 5/8-in. DT Energy Values (RW Orientation, Machined-Notch Crack Starters) From a 12-in. A533-B Steel Plate (HSST 03)

Location (see Fig. 12)	Temperature		Specimen Number		DT Energy (ft-lb)		Location (see Fig. 12)	Temperature		Specimen Number		DT Energy (ft-lb)				
	°F	°C	In Top Half of Plate	In Bottom Half of Plate	In Top Half of Plate	In Bottom Half of Plate		°F	°C	In Top Half of Plate	In Bottom Half of Plate	In Top Half of Plate	In Bottom Half of Plate			
A	-120	-84	N36-A1	N36-A28	65	63	E	120	49	N36-E9	N36-E23	485	483			
	-100	-73		N36-A15		62				N36-E5		469				
	-80	-62	N36-A2		87				140	60	N36-E10	N36-E24	759	685		
	-60	-51	N36-A9	N36-A16	256	224					N36-E19		667			
				N36-A23		184			160	71	N36-E11	N36-E25	968	928		
	-40	-40	N36-A10	N36-A24	430	342							1024			
			N36-A3		321				180	82		N36-E20		1012		
	-20	-29	N36-A11	N36-A25	930	763					N36-E12	N36-E26	1056	983		
			N36-A14	N36-A17	880	397					N36-E13	N36-E27	1072	1030		
	0	-18	N36-A6	N36-A26	1005	832			200	93	N36-E7		1075			
			N36-A12		957											
	20	-7	N36-A13	N36-A27	951	969			220	104		N36-E21		957		
				N36-A18		975			240	116	N36-E14	N36-E28	1033	1038		
	40	4	N36-A5	N36-A22	933	992		F	-40	-40	N36-F1			57		
			N36-A8		922					-20	-29		N36-F15		84	59
	60	16		N36-A19		981				0	-18	N36-F2				
	80	27	N36-A4		1075	987				20	-7		N36-F16		126	106
	100	38		N36-A20		987				40	4	N36-F3			126	170
	120	49	N36-A7	N36-A21	1008	987				60	16		N36-F17		245	
	200	93								80	27	N36-F4		308	360	
							100		38	N36-F8	N36-F18		370			
										N36-F5	N36-F22		436	474		
							120		49	N36-F9	N36-F23		460			
B	-80	-62	N36-B1		57			140	60	N36-F10	N36-F24		577			
	-60	-51		N36-B15		60				N36-F19	N36-F25		574			
	-40	-40	N36-B2	N36-B16	187	115		160	71	N36-F11	N36-F26	1051	888			
	-20	-29								N36-F6		950				
	0	-18	N36-B3	N36-B17	187	211		180	82	N36-F12	N36-F27	1019	946			
	20	-7								N36-F20		1017				
	40	4	N36-B5		350			200	93	N36-F13	N36-F27	1030	953			
			N36-B8		354					N36-F7		1049				
	60	16	N36-B9	N36-B18	469	410		220	104	N36-F14	N36-F21	1012	965			
	80	27	N36-B10	N36-B23	654	541		240	116		N36-F28		1075			
C	100	38	N36-B4	N36-B24	604	872	G	-40	-40	N36-G1			52			
	120	49	N36-B11	N36-B19	925	818			-20	-29		N36-G15		60	56	
			N36-B12	N36-B25	1051	1044			0	-18	N36-G2					
	140	60	N36-B6	N36-B26	1039	1010			20	-7		N36-G16		127	99	
			N36-B13	N36-B20	1115	972			40	4	N36-G3			187		
	160	71	N36-B7		1026				60	16		N36-G17		236	187	
	180	82		N36-B21		1083			80	27	N36-G4			345		
	200	93	N36-B14	N36-B27	1032	1051			100	38		N36-G18		423	447	
	220	104		N36-B28		1024			120	49	N36-G5	N36-G22	423	447		
									140	60	N36-G8		445			
D	-40	-40	N36-C1		56					N36-G9	N36-G23	551	596			
	-20	-29		N36-C15		62		160	71	N36-G10	N36-G19	837	875			
	0	-18	N36-C2		108	159				N36-G6		869				
	20	-7		N36-C16		159		180	82	N36-G11	N36-G25	962	887			
	40	4	N36-C3		179	253				N36-G12	N36-G20	981	966			
	60	16		N36-C17		253		200	93	N36-G7	N36-G26	962	935			
	80	27	N36-C4	N36-C22	404	306		220	104	N36-G13	N36-G21	1039	944			
	100	38	N36-C8	N36-C18	475	481		240	116		N36-G27		1011			
				N36-C28		439		260	127	N36-G14	N36-G28	959	1027			
	120	49	N36-C9	N36-C23	660	690	H	-40	-40	N36-H1			54			
140	60	N36-C5		755				-20	-29		N36-H15		60			
160	71	N36-C10	N36-C19	935	962			0	-18	N36-H2		81				
180	82		N36-C24		956			20	-7		N36-H16		139	106		
		N36-C6	N36-C25	1038	1013			40	4	N36-H3			215			
200	93	N36-C7	N36-C20	1027	960			60	16		N36-H17		281			
220	104	N36-C13	N36-C26	1077	985			80	27	N36-H4			329			
240	116	N36-C14	N36-C27	971	1028			100	38		N36-H18		461			
			N36-C21	1009	1076			120	49		N36-H22		423	485		
										N36-H5		461				
E	-40	-40	N36-D1	N36-D15	51	60		140	60	N36-H9	N36-H19	584	627			
	-20	-29								N36-H23		605				
	0	-18	N36-D2	N36-D16	91	114		160	71	N36-H10	N36-H24	949	949			
	20	-7								N36-H6		907				
	40	4	N36-D3	N36-D17	156	216		180	82	N36-H11	N36-H20	997	931			
	60	16		N36-D18		385				N36-H12	N36-H25	959				
	80	27	N36-D4	N36-D28	310	374		200	93		N36-H26	967	976			
	100	38	N36-D8	N36-D22	455	601				N36-H7		905				
	120	49	N36-D5		549	679		220	104		N36-H21		990			
	140	60	N36-D13	N36-D19	544	623				N36-H13	N36-H27	1014	988			
F	160	71	N36-D6	N36-D24	907	1050	I	-120	-84	N36-I14			52			
	180	82	N36-D10	N36-D25	1008	1075			0	-18	N36-I1		60			
			N36-D11	N36-D20	1013	1036			40	4	N36-I2		139			
	200	93	N36-D7	N36-D26	1002	1028			80	27	N36-I3		309			
	220	104	N36-D12	N36-D21	1025	999			100	38	N36-I10		340			
	240	116		N36-D27		1056			120	49	N36-I4		501			
	260	127	N36-D14		1023				140	60	N36-I9		642			
									160	91	N36-I5		915			
											N36-I11		855			
									180	82	N36-I8		931			
							200	93	N36-I12		981					
									N36-I13		933					
							220	104	N36-I6		962					
									N36-I7		1003					

Table A4
Data Plotted in Fig. 15: 5/8-in. DT Energy Values From a 12-in. A533-B Class 1 Plate (HSST 01) in the RW Orientation at Elevated Temperature (Specimens From Location D in Fig. 7 From the Bottom Half of the Plate Thickness and With EB-Weld Crack Starters

Temperature		Specimen Number	DT Energy (ft-lb)
°F	°C		
200	93	L-74-H1	1150
220	104	L-74-H4	1100
250	121	L-74-H3	1082
300	149	L-74-H5, L-74-H6	1149, 1176
350	177	L-74-H7, L-74-H8	1149, 1070
400	204	L-74-H9, L-74-H10	1318, 1360
450	232	L-74-H15, L-74-H12	1280, 1265
500	260	L-74-H13, L-74-H14	1321, 1259
550	288	L-74-H15, L-74-H16	1250, 1157
600	316	L-74-H2	1071

Table A5
Data Plotted in Figs. 16 and 18: 5/8-in. DT Energy Values for a 6-in. A533-B Class 2 Steel Plate

Location (see Fig. 16)	Temperature		Specimen Number*	DT Energy (ft-lb)	Location (see Fig. 16)	Temperature		Specimen Number*	DT Energy (ft-lb)	Location (see Fig. 16)	Temperature		Specimen Number*	DT Energy (ft-lb)		
	°F	°C				°F	°C				°F	°C				
RW Orientation, Machined Notch				RW Orientation, Machined Notch				RW Orientation, EB Weld								
A	-50	-46	L-14-A11	222*	D	-20	-29	L-14-D11	97*	C	80	27	L-14-C10	592		
	-50	-46	L-14-A4	54		0	-18	L-14-D4	194		100	38	L-14-C18	690		
	-27	-33	L-14-A5	64		20	-7	L-14-D12	192		120	49	L-14-C15	925*		
	0	-18	L-14-A12	201		40	4	L-14-D6	420		160	71	L-14-C16	984		
	0	-18	L-14-A13	298*		60	16	L-14-D13	357*		200	93	L-14-C17	1135*		
	0	-18	L-14-A2	538*		74	23	L-14-D1	441*		D	-20	-29	L-14-D7	77*	
	40	4	L-14-A6	336		80	27	L-14-D22	479			20	-7	L-14-D8	159	
	50	10	L-14-A22	695		100	38	L-14-D14	782			60	16	L-14-D9	554*	
	50	10	L-14-A21	683*		120	49	L-14-D2	978*			80	27	L-14-D18	521	
	74	23	L-14-A1	902*		120	49	L-14-D21	790*			100	38	L-14-D10	904	
	100	38	L-14-A19	967*		140	60	L-14-D19	837*			120	49	L-14-D17	920*	
	100	38	L-14-A14	934		160	71	L-14-D3	927*			140	60	L-14-D15	933*	
	120	49	L-14-A3	980*		180	82	L-14-D20	826			180	82	L-14-D16	904	
	160	71	L-14-A20	1031		200	93	L-14-D5	955			E	60	16	L-14-E4	344
B	-40	-40	L-14-B12	132	E	60	16	L-14-E6	460	100			38	L-14-E8	562	
	-25	-32	L-14-B5	95		74	23	L-14-E2	666*	140			60	L-14-E5	848	
	0	-18	L-14-B3	323*		100	38	L-14-E10	671	160			71	L-14-E9	845*	
	0	-18	L-14-B11	232*		140	60	L-14-E7	824*	WR Orientation, EB Weld						
	38	3	L-14-B6	325		160	71	L-14-E3	915*	C			20	-7	L-14-C6	179
	40	4	L-14-B14	424		160	71	L-14-E11	730*		40		4	L-14-C12	235	
	74	23	L-14-B1	720*		RW Orientation, EB Weld					60		16	L-14-C5	342*	
	80	27	L-14-B13	648*		A	-50	-46	L-14-A7		141*		80	27	L-14-C11	394*
	100	38	L-14-B21	1084			0	-15	L-14-A9		292*		100	38	L-14-C4	592
	120	49	L-14-B20	1070			0	-18	L-14-A8		163		120	49	L-14-C10	735
	120	49	L-14-B6	737			50	10	L-14-A18		650		140	60	L-14-C3	653*
	160	71	L-14-B4	1081			50	10	L-14-A17		500*		160	71	L-14-C9	684*
	160	71	L-14-B19	1101*			100	38	L-14-A15		880*		180	82	L-14-C2	666*
	200	93	L-14-B22	1048			100	38	L-14-A10		1076	180	82	L-14-C14	689	
C	-40	-40	L-14-C11	65*	160		71	L-14-A16	918		200	93	L-14-C7	738*		
	0	-18	L-14-C12	127	B		-40	-40	L-14-B8		61	200	93	L-14-C8	741	
	0	-18	L-14-C5	123*			0	-18	L-14-B7		113*	220	104	L-14-C13	656*	
	40	4	L-14-C2	364			40	4	L-14-B10		349	220	104	L-14-C1	667*	
	40	4	L-14-C13	292*			80	27	L-14-B9	812*	E	80	27	L-14-E1	502*	
	74	23	L-14-C1	750*			100	38	L-14-B17	696*		100	38	L-14-E7	714*	
	80	27	L-14-C14	538			120	49	L-14-B16	705		120	49	L-14-E6	661	
	100	38	L-14-C22	642		160	71	L-14-B15	1085*	140		60	L-14-E5	642*		
	120	49	L-14-C4	979		200	93	L-14-B18	1139	160		71	L-14-E4	660		
	120	49	L-14-C19	992*		C	-40	-40	L-14-C7	60*		180	82	L-14-E3	671*	
	160	71	L-14-C3	993*			0	-18	L-14-C8	75		200	93	L-14-E2	654*	
	160	71	L-14-C20	927			40	4	L-14-C9	221*						
	160	71	L-14-C4	1022												
	200	93	L-14-C21	947												

*The DT energy values marked with an asterisk are those from specimens cut from the top surface to the midthickness (from the right of the sketch in Fig. 16).

Table A6
Data Plotted in Fig. 19: 5/8-in. DT Energy Values (EB-Weld Crack Starters)
From a 12-in. Submerged Arc Weld Formed With A533 Steel (HSST Plate 01;
HSST Weld 50)

Location (see Fig. 19)	Temperature		Specimen Number	DT Energy (ft-lb)	Location (see Fig. 19)	Temperature		Specimen Number	DT Energy (ft-lb)
	°F	°C				°F	°C		
A	0	-18	N-31-A6	166	G	20	-7	N-31-G4	277
	80	27	N-31-A5	760		80	27	N-31-G5	1124
	120	49	N-31-A4	1245		80	27	N-31-G6	1545
B	0	-18	N-31-B6	170	H	-20	-29	N-31-H4	198
	40	4	N-31-B1	762		20	-7	N-31-H2	193
	80	27	N-31-B4	1281		60	16	N-31-H5	1043
	120	49	N-31-B2	1515		100	38	N-31-H3	923
	160	71	N-31-B5	1342		100	38	N-31-H6	1324
	200	93	N-31-B3	1440		140	60	N-31-H1	1318
C	-40	-40	N-31-C1	101	I	60	16	N-31-I1	663
	0	-18	N-31-C4	148		100	38	N-31-I2	1116
	40	4	N-31-C2	461		120	49	N-31-I3	1256
	60	16	N-31-C6	751	Ⓐ	60	16	N-31-TA2	325
	80	27	N-31-C5	1260	100	38	N-31-TA1	772	
D	120	49	N-31-C3	1343	Ⓑ	60	16	N-31-TB1	1035
	-40	-40	N-31-D5	108	80	27	N-31-TB2	1226	
	0	-18	N-31-D1	203	Ⓒ	20	-7	N-31-TC1	169
	20	-7	N-31-D3	318	80	27	N-31-TC2	575	
	40	4	N-31-D4	402	Ⓓ	60	16	N-31-TD1	516
	60	16	N-31-D6	943	100	38	N-31-TD2	578	
E	80	27	N-31-D2	1278	Ⓔ	40	4	N-31-TE2	348
	0	-18	N-31-E4	130	80	27	N-31-TE1	732	
	60	16	N-31-E6	1198	Ⓕ	40	4	N-31-TF1	382
F	80	27	N-31-E5	1281	60	16	N-31-TF2	725	
	-20	-29	N-31-F4	148	Ⓖ	40	4	N-31-TG1	147
	80	27	N-31-F5	1483	80	-18	N-31-TG2	1362	
	80	27	N-31-E4	1434		80	27		

Table A7
Data Plotted in Fig. 21: 5/8-in. DT Energy Values (EB-Weld Crack
Starters) From a 6-in. Electroslag Weld Formed With A533 Steel
(HSST Weld 53)

Location (see Fig. 19)	Temperature		Specimen Number	DT Energy (ft-lb)
	°F	°C		
Top Weld Surface				
A	40	4	N66-A4	275
	80	27	N66-A3	381
	100	38	N66-A2	800
	200	93	N66-A1	742
Bottom Weld Surface				
A	0	-18	N66-A5	173
	100	38	N66-A7	527
	120	49	N66-A6	650
	150	66	N66-A8	703

Table A8
Data Plotted in Fig. 22: 1-in. DT Energy Values From a 12-in. A533-B
Class 1 Steel Plate (HSST 01) in the RW Orientation (EB-Weld Crack
Starters)

Loca- tion (see Fig. 22)	Temper- ature		Specimen Number*	DT Energy (ft-lb)	Loca- tion (see Fig. 22)	Temper- ature		Specimen Number*	DT Energy (ft-lb)
	°F	°C				°F	°C		
A	-80	-62	L-74-VA2	398	C	180	82	L-74-VC9	7800*
	-60	-51	L-74-VA3	705*		200	93	L-74-VC10	7610
	-40	-40	L-74-VA4	1092		220	104	L-74-VC11	7310*
	-20	-29	L-74-VA5	1234*	D	-40	-40	L-74-VD1	466*
	0	-18	L-74-VA6	881		0	-18	L-74-VD2	331
	20	-7	L-74-VA7	5452*		40	4	L-74-VD3	811*
	20	-7	L-74-VA1	4640*		80	27	L-74-VD4	1948
	40	4	L-83-VA2	5748		100	38	L-74-VD5	2446*
	60	16	L-83-VA1	7436*		120	49	L-74-VD6	3785
	80	27	L-74-VA9	7710*		120	49	L-74-VD12	3752
	120	49	L-74-VA10	8430		140	60	L-83-VD1	7040*
140	60	L-74-VA11	7900*	140		60	L-74-VD7	7610*	
B	-80	-62	L-74-VB1	398*		160	71	L-74-VD8	9050
	-40	-40	L-74-VB2	398	160	71	L-83-VD2	6678	
	0	-18	L-74-VB3	398*	180	82	L-74-VD9	9390*	
	40	4	L-74-VB4	1376	200	93	L-74-VD10	7990	
	60	16	L-74-VB5	1305*	220	104	L-74-VD11	7210*	
	80	27	L-74-VB6	2516	E	-40	-40	L-74-VE1	466*
	80	27	L-83-VB2	2853		0	-18	L-74-VE2	500
	100	38	L-83-VB1	4890*		40	4	L-74-VE3	881*
	100	38	L-74-VB7	4966*		80	27	L-74-VE4	1519
	120	49	L-74-VB8	6680		100	38	L-74-VE5	2864*
	120	49	L-74-VB12	5986		120	49	L-74-VE6	4479
140	60	L-74-VB9	7800*	140		60	L-74-VE7	6900*	
160	71	L-74-VB10	7610	160	71	L-74-VE8	6460		
180	82	L-74-VB11	7990*	160	71	L-74-VE12	7118		
C	-40	-40	L-74-VC1	398*	180	82	L-74-VE9	7100*	
	0	-18	L-74-VC2	433	200	93	L-74-VE10	7410	
	40	4	L-74-VC3	951*	220	104	L-74-VE11	8260*	
	80	27	L-74-VC4	2091	F	80	27	L-74-VF1	1948*
	100	38	L-74-VC5	3069*		120	49	L-74-VF3	4479*
	100	38	L-83-VC2	3239		140	60	L-83-VE1	6452*
	120	49	L-83-VC1	3624*		160	71	L-74-VF5	6570*
	120	49	L-74-VC6	4479		180	82	L-74-VF7	6570*
	140	60	L-74-VC7	7410*		200	93	L-74-VF9	7100*
	140	60	L-74-VC12	7040		220	104	L-74-VF11	5890*
	160	71	L-74-VC8	8600					

*The DT energy values marked with an asterisk are those from specimens cut from the top surface to the midthickness.

Table A9
Data Plotted in Fig. 23: 1-in. DT Energy Values From a
6-in. A533-B Class 2 Steel Plate in the RW Orientation

Location (see Fig. 22)	Temperature		Specimen Number	DT Energy (ft-lb)
	°F	°C		
A: Top surface	40	4	L-14-44A	2554
	75	24	L-14-42B	4114
	90	32	L-14-42A	7128
	100	38	L-14-44B	7078
	120	49	L-14-44D	8646
	140	60	L-14-42D	9980
	160	71	L-14-42C	6973
	200	93	L-14-44C	6969
B: Between top surface and midthickness	40	4	L-14-44I	1408
	75	24	L-14-42J	2430
	90	32	L-14-42I	4820
	100	38	L-14-44J	6022
	120	49	L-14-44L	8352
	140	60	L-14-42L	6300
	160	71	L-14-42K	9096
	200	93	L-14-44K	7100
C: Midthickness	40	4	L-14-44E	2925
	75	24	L-14-42F	2796
	90	32	L-14-42E	6500
	100	38	L-14-44F	6420
	120	49	L-14-44H	6025
	140	60	L-14-42H	5860
	160	71	L-14-42G	7220
	200	93	L-14-44G	6831

Table A10
Data Plotted in Fig. 24: 3-in. DT Energy Values From a
12-in. A533-B Class 1 Steel Plate (HSST 01)

Location	Temperature		Specimen Number	DT Energy (ft-lb)	Location	Temperature		Specimen Number	DT Energy (ft-lb)
	°F	°C				°F	°C		
RW Orientation					WR Orientation				
Surface	-40	-40	L-83-X3C	4600	Surface	120	49	L-74-TW6	24400
	0	-18	L-83-X1A	5350		140	60	L-74-TW5	34200
	40	4	L-83-X3B	9940		160	71	L-74-TW3	40800
	80	27	L-83-X1B	14500		180	82	L-74-TW2	49500
	100	38	L-83-X3A	17170		220	104	L-74-TW1	53200
	120	49	L-83-X3	30800	1/2 T	160	71	L-74-CW3	25800
	140	60	L-83-X1C	50000		180	82	L-74-CW2	31700
	160	71	L-74-TR6	69300		212	100	L-74-CW1	35000
	180	82	L-74-TR5	72700					
	200	93	L-74-TR2	> 75200					
212	103	L-74-TR3	> 77000						
240	116	L-74-TR1	> 80500						
1/2 T	80	27	L-83-X2B	4580					
	120	49	L-83-X2C	11200					
	140	60	L-83-X2A	17300					
	160	71	L-83-X2D	38600					
	180	82	L-74-CR2	45700					
	220	104	L-74-CR1	49600					

Table A11

Data Plotted in Fig. 25: 3-in. DT Energy Values From a 6-in. A533-B Class 2 Steel Plate (Each Specimen Spanning From the Surface to Midthickness)

Temperature		Specimen Number	DT Energy (ft-lb)
°F	°C		
RW Orientation			
0	-18	L-14-42	3120
73	23	L-14-44	9500
120	49	L-14-41	16750
160	71	L-14-41Y	50600
200	93	L-14-43Y	60920
265	129	L-14-43Z	62660
WR Orientation			
205	96	L-14-75	31650
262	128	L-14-76	32200

Table A12

DT Energy Values From a 6-in. A533-B Class 2 Steel Plate Using Special 3-in. Specimens Geometrically Similar to the 5/8-in. DT Specimen and Spanning From the Surface to Midthickness (RW Orientation)

Temperature		Specimen Number	DT Energy (ft-lb)
°F	°C		
195	91	L-14-71	62600
263	128	L-14-72	59820

Table A13

Data Plotted in Fig. 27: 6-in. DT Energy Values From a 6-in. A533-B Class 2 Steel Plate

Orientation	Temperature		Specimen Number	DT Energy (ft-lb)
	°F	°C		
RW	70	21	L-14-4	49600
	120	49	L-14-5	63600
	170	77	L-14-3	>161000
WR	40	4	L-14-12	16800
	75	24	L-14-7	17400
	140	60	L-14-8	66100
	160	71	L-14-6	134500

Table A14

Data Plotted in Fig. 30: 12-in. DT Energy Values From a 12-in. A533-B Class 1 Steel Plate (HSST 01) With the Specimens Oriented in the RW Direction

Temperature		Specimen Number	DT Energy (ft-lb)
°F	°C		
30	-1	1D	59000
100	38	1E	155000
150	66	1C	290000
180	82	1G	446000
216	103	1F	>769000

